Closed-Loop Identification of Sparse Networked Systems

ETH
Eidgenössische Technische Hochschule Zürich
Swiss Federal Institute of Technology Zurich

IFA Automatic Control Laboratory

Master's Thesis

Closed-Loop Identification of Sparse Networked Systems

Ran Chen
September 12, 2023

Supervisors
Prof. Dr. Roy S. Smith
Dr. Amber Srivastava
Mingzhou Yin

Contents

Abstract

In this project, we extend the application of two typical closed-loop identification methods, namely the dual-Youla parameterization and the two-stage identification, from identifying LTI SISO systems to MIMO systems while considering the predefined sparsity structure in the system. Both extended methods result in a quadratic program that consists of 1) a quadratic cost function that minimizes the model fitting error, and 2) a group of linear equality constraints that ensure the estimated system has the desired sparsity structure. These two methods are applicable in distinct scenarios. In particular, the dual-Youla method requires the knowledge of the controller and guarantees the estimated plant is stabilized by the known controller, whereas the two-stage method does not rely on the controller's knowledge. Both methods are proven to admit a consistent estimate of the plant theoretically. Finally, to showcase the practical efficacy of the proposed method, we apply our approach to identifying an inherently unstable and sparse irrigation networked system directly using closed-loop noisy data. Given the inherent instability of the irrigation network, we exclusively employ the extended dual-Youla method, as it guarantees stabilizability.

Chapter 1

Introduction

System identification, the methodology employed for constructing reliable system models based on empirical data, has found extensive application in engineering[1], as it forms an essential step in facilitating model-based control design[2], minimum variance control design[3], robust control design[4], and so on. Nonetheless, conventional approaches in system identification typically center around the estimation of individual parameters, without effectively capturing the a-priori knowledge about the system's underlying architecture. The problem gains increased relevance within the context of contemporary cyber-physical systems (CPS), which can exhibit large-scale sparse architectures, where both the system and the controller can only access localized information. These systems are common in many fields, such as integrated propulsion systems, power grids, vehicle platoons, and irrigation networks[5][6], usually faced with the difficulty in generating a representative model for controller synthesis, owing to factors like heterogeneity, concurrency, or susceptibility to temporal intricacies[7]. Moreover, large-scale systems may demonstrate undesired dynamics; for instance, power grids with continuously increasing demand may rely on intensive usage of the existing networks, incurring smaller stability margins and even instability under poorly damped dynamics[8]. This indicates that these systems almost always operate in closed-loop configurations, thereby rendering exclusively closed-loop data available for identification purposes. Consequently, it becomes imperative to develop novel techniques that are tailored for closed-loop identification of the CPS that make effective use of sparsity knowledge to further improve the identification of the system.

It is widely recognized that a main challenge in closed-loop identification stems from the correlation between the unobservable noise and the control input, which employs the noisy output as feedback. Such problems have raised great interest in the literature. By convention, approaches for closed-loop identification are referred to as indirect methods, as opposed to the direct methods that address open-loop identification problems. Thus, this project primarily centers around extending two traditional indirect methods: the dual-Youla parameterization[9] and the two-stage identification[10]. These frameworks are the focal points of our investigation and are adaptable to distinct scenarios. At the same time, both can be tailored to facilitate the identification of large-scale systems with certain sparsity architectures.

The dual-Youla method parameterizes a set of systems stabilized by a known controller, indicating every resultant estimate via the dual-Youla method is guaranteed to be stabilized by the controller. Such stabilizability relies on the coprime factorization of the controller, which is particularly beneficial when the original system is unstable or possesses a limited stability margin. The procedure of this method involves filtering the raw input and output data using these coprime factors to generate a new signal pair, interpreted as the virtual input and virtual output. Notably, the virtual input becomes uncorrelated with noise, making the problem solv-

able by an open-loop identification framework.

In contrast, in situations where exact controller knowledge is absent or determining the coprime factors of the controller is challenging, an alternative indirect method called the two-stage method becomes attractive. In the first stage, this method estimates the sensitivity function from the reference signal to the control input. This estimated sensitivity function is then used to filter the reference signal, resembling the noise-free part of the control input. Subsequently, this noise-free control input, along with the raw output, is employed to identify the plant as an open-loop identification problem, since noise-free input is uncorrelated by noise. Implementing the two-stage method is simple due to its lack of reliance on coprime factorization or exact controller knowledge. However, this simplicity comes with a price: the identified plant is not guaranteed to be stabilized by the controller, rendering it less desirable for identifying unstable plants.

While these two approaches are inherently suited for different scenarios, it is worth noting that they share the capacity to be customized for large-scale sparse systems, provided knowledge of the sparsity architectures is available. As this specific adaptation has not been extensively explored in the existing literature, the potential of incorporating sparsity conditions into the identification framework emerges as a valuable investigation. With this purpose, the utilization of the sparsity structure knowledge is realized through the so-called Sparsity Invariance Theorem[11], which was initially applied in controller synthesis. The theorem introduces a group of linear constraints, namely the sparsity constraints, on the factors of a transfer matrix to indirectly ensure the transfer matrix showcases the desired sparsity configuration so that the optimization problem remains convex.

As motivated by the theories and concepts above, the main contribution of this project is introducing an innovative concept that integrates the Sparsity Invariance Theorem into the conventional system identification frameworks mentioned previously. The extended methods ultimately result in an efficiently solvable quadratic program, allow for a closed-form solution, and guarantee the estimated plant has exactly the desired sparsity architecture. Consistency proof is also provided, followed by the implementation. Finally, simulations demonstrate that a consistent output prediction and a commendable model approximation are achievable and increasingly efficient compared to the traditional identification method that ignores the sparsity knowledge.

The structure of this report is organized as follows. Chapter 2 provides a general overview of the essential mathematical preliminaries, which outlines the system identification framework before introducing the notations and theorems that will be extensively referenced throughout the report. In Chapter 3 and Chapter 4, the extended dual-Youla method and two-stage method are elaborated, respectively, by introducing the fundamental principles of these two conventional identification frameworks and adapting their methodologies to the Sparsity Invariance Theorem, before converting the identification problem into a quadratic program. Moving to Chapter 5, an instance of applying our proposed method to a real-world scenario is illustrated by identifying an inherently unstable and sparse irrigation network directly through closed-loop data, followed by a discussion about several directions that could potentially improve the estimate in the future. Finally, in Chapter 6, a summary of the findings is presented, and the overall conclusions are drawn.

Chapter 2

Preliminaries

This chapter serves as a foundation for the subsequent discussions in this report. In this chapter, we present an overview of the mathematical tools and concepts that will be frequently used throughout the report. We begin by introducing the problem statement regarding the general framework of systems involved in this report, followed by a summary of the notations employed in various chapters and summarized in Section 2.1 and 2.2, respectively. Additionally, in Section 2.3, we delve into essential theorems from the literature and develop certain new concepts that assist in building the mathematical model. These theorems lay the groundwork for understanding the convexification of several tricky constraints and formulating optimization problems.

2.1 Problem Statement

We consider a general linear time-invariant (LTI) multi-input multi-output (MIMO) system with a positive feedback controller in discrete time with a block diagram displayed in Fig.2.1,

$$\begin{aligned} y(k) &= \mathbf{G}(z)u(k) + \mathbf{H}(z)e(k) \\ u(k) &= \mathbf{K}(z)y(k) + \mathbf{F}(z)r(k) \end{aligned} \tag{2.1}$$

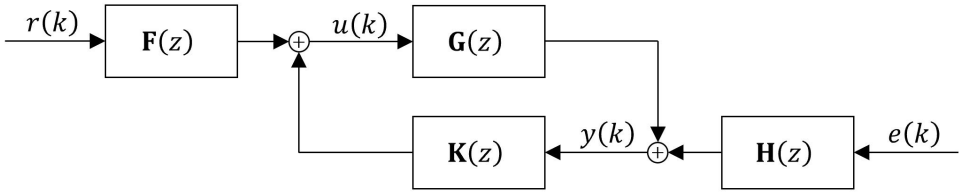

Figure 2.1: Block diagram of an LTI feedback control system incorporating error and excitation.

The dynamics consist of vectors of measured outputs $y(k) \in \mathbb{R}^{n_y}$, measurement noises $e(k) \in \mathbb{R}^{n_e}$, control inputs $u(k) \in \mathbb{R}^{n_u}$, and external excitation $r(k) \in \mathbb{R}^{n_r}$. The matrices of transfer functions $\mathbf{G}(z) \in \mathcal{R}_c^{n_y \times n_u}$, $\mathbf{H}(z) \in \mathcal{R}_c^{n_y \times n_e}$, $\mathbf{K}(z) \in \mathcal{R}_c^{n_u \times n_y}$ and $\mathbf{F}(z) \in \mathcal{R}_c^{n_u \times n_r}$ represent the input-output (IO) plant, the noise dynamics, the positive feedback controller and the excitation pre-filter, respectively. The notation $\mathcal{R}_c^{m \times n}$ represents the field of $m \times n$ causal transfer matrices. Specifically, the MIMO plant $\mathbf{G}(z)$ demonstrates the structure below,

$$\mathbf{G}(z) = \begin{bmatrix} G_{11}(z) & G_{12}(z) & \cdots & G_{1n_u}(z) \\ G_{21}(z) & G_{22}(z) & \cdots & G_{2n_u}(z) \\ \vdots & \vdots & \ddots & \vdots \\ G_{n_y1}(z) & G_{n_y2}(z) & \cdots & G_{n_yn_u}(z) \end{bmatrix} \tag{2.2}$$

Each $G_{ij} \in \mathcal{R}_c$ represents a rational transfer function. Besides, we consider the following fundamental assumptions:

1). $r(k)$ is persistently exciting.

2). $e(k)$ is unobservable, independent and identically distributed (i.i.d.), and statistically independent of $r(k)$.

3). The plant is identifiable; the network structure is exactly known, or it is also identifiable[12].

Which together ensure the identification problem is generally solvable. The problems we consider in this report are identical to conventional ones in the literature, which aims at estimating all the parameters of each IO channel $G_{ij}(z)$, by utilizing the pre-selected excitation, control input and the noise-corrupted output. Additionally, the extended dual-Youla method described in Chapter 3 requires the knowledge of the controller $\mathbf{K}(z)$.

2.2 Nomenclatures

To ensure uniformity in notation and facilitate readers in promptly grasping the symbols, we provide a condensed compilation of the symbols and operators in the table below.

Table 2.1: Nomenclature

Symbol	**Representation**	**Remark**
$\mathbb{R}$	Fields of real numbers	$\mathbb{R}^{m\times n} = m \times n$ real matrix
$\mathbb{C}$	Fields of complex numbers	
$\{0,1\}^{m\times n}$	Fields of $m \times n$ binary matrices	
$\mathcal{R}_c$	Fields of causal transfer functions	$\mathcal{R}_c^{m\times n} = m \times n$ transfer matrix
$\mathcal{RH}_\infty$	Fields of stable and causal transfer functions	
$\mathcal{F}_\tau$	Fields of FIR transfer functions with order τ	
$\mathbf{A}(s)$	Transfer function in continuous-time	Bold symbols w. (s)
$\mathbf{A}$ or $\mathbf{A}(z)$	Transfer function in discrete-time	Bold symbols w. or w/o. (z)
A^k	a real matrix equal to k-th tap of $\mathbf{A}$	Superscripts
$A_{ij}(z)$	a transfer function equal to (i,j)-entry of $\mathbf{A}$	Subscripts
a_{ij}^k	(i,j)-entry of the k-th tap of $\mathbf{A}$	Super- and subscripts
I_n	Identity matrix with dimension n	
$\mathbf{0}$	Zero matrix with proper size based on context	
$\mathbb{1}^{m\times n}$	An $m \times n$ matrix with all elements equal to 1	
$A^\top$	Transpose of A	
$A^\dagger$	Pseudo-inverse of A	
$A \bigotimes B$	Kronecker product of two matrices A and B	
z^{-1}	Shift operator in discrete-time	$z^{-1} \cdot y(k) = y(k-1)$
$\exp(\tau)$	Natural exponentiation of τ, i.e. e^τ	
$\mathbf{vec}(B)$	Vectorization operator	Detailed definition below
$\mathbf{toep}(\mathbf{B}, \nu)$	Toeplitz operator with ν rows	Detailed definition below
Sparse(S)	Sparsity subspace w.r.t. binary S	Detailed definition below
Struct$(\mathbf{B})$	Sparsity structure of $\mathbf{B}$	Detailed definition below

The vectorization operator is defined by stacking every column of a matrix to form another long vector. Suppose we are given a matrix $B \in \mathbb{R}^{m\times n}$ such that,

$$B = \begin{bmatrix} b_{11} & b_{12} & \cdots & b_{1n} \\ b_{21} & b_{22} & \cdots & b_{2n} \\ \vdots & \vdots & \ddots & \vdots \\ b_{m1} & b_{m2} & \cdots & b_{mn} \end{bmatrix} = \begin{bmatrix} \mathbf{b}_1 & \mathbf{b}_2 & \cdots & \mathbf{b}_n \end{bmatrix} \tag{2.3}$$

Hence,

$$\mathbf{vec}(B) = \begin{bmatrix} \mathbf{b}_1 \\ \mathbf{b}_2 \\ \vdots \\ \mathbf{b}_n \end{bmatrix} \in \mathbb{R}^{mn} \tag{2.4}$$

The Toeplitz operator in this report is exclusively defined for an FIR transfer matrix. Suppose we are given a transfer matrix $\mathbf{B}(z) \in \mathcal{F}_\tau^{m\times n}$ such that,

$$\begin{aligned} \mathbf{A}(z) &= A^0 + A^1 \cdot z^{-1} + \cdots + A^{\nu-1} \cdot z^{-(\nu-1)} \\ \mathbf{B}(z) &= B^0 + B^1 \cdot z^{-1} + \cdots + B^{\tau-1} \cdot z^{-(\tau-1)} \end{aligned} \tag{2.5}$$

Further, suppose we are given another FIR transfer matrix $\mathbf{A}(z) \in \mathcal{F}_\nu$ with proper dimensions and we want to perform the convolution $\mathbf{A}(z) \cdot \mathbf{B}(z)$. We first define $\mathbf{toep}(\mathbf{B}, \nu)$ as,

$$\mathbf{toep}(\mathbf{B}, \nu) = \begin{bmatrix} B^0 & B^1 & \cdots & B^{\tau-1} & \mathbf{0} & \cdots & \mathbf{0} \\ \mathbf{0} & B^0 & \cdots & B^{\tau-2} & B^{\tau-1} & \cdots & \mathbf{0} \\ \vdots & \vdots & \ddots & \vdots & \vdots & \ddots & \vdots \\ \mathbf{0} & \mathbf{0} & \cdots & B^0 & B^1 & \cdots & B^{\tau-1} \end{bmatrix} \in \mathbb{R}^{m\cdot\nu\times N\cdot(\tau+\nu-1)} \tag{2.6}$$

Therefore, the Toeplitz operator converts the convolution into the following equivalent matrix multiplication,

$$\begin{aligned} &\mathbf{A}(z) \cdot \mathbf{B}(z) \text{ is computed via} \\ &\begin{bmatrix} A^0 & A^1 & \cdots & A^{\nu-1} \end{bmatrix} * \begin{bmatrix} B^0 & B^1 & \cdots & B^{\tau-1} \end{bmatrix} \\ =&\begin{bmatrix} A^0 & A^1 & \cdots & A^{\nu-1} \end{bmatrix} \cdot \mathbf{toep}(\mathbf{B}, \nu) \end{aligned} \tag{2.7}$$

Finally, Sparse$(\cdot)$ and Struct$(\cdot)$ are defined in the same way as those in [11]. Given a binary matrix $S \in \{0,1\}^{m\times n}$,

$$\text{Sparse}(S) = \{\mathbf{B} \in \mathcal{R}_c^{m\times n} \mid B_{ij}(z)\ \forall\ z \in \mathbb{C} \text{ and } \forall\ i,j \text{ s.t. } S_{ij} = 0\} \tag{2.8}$$

On the other hand, given a causal transfer matrix $\mathbf{B} \in \mathcal{R}_c^{m\times n}$, the binary matrix $S = \text{Struct}(\mathbf{B})$ is defined as,

$$S_{ij} = \begin{cases} 0 \text{ if } B_{ij}(z) = 0\ \forall\ z \in \mathbb{C} \\ 1 \text{ otherwise} \end{cases} \tag{2.9}$$

2.3 Related Theorems

This section describes all relevant theorems used to construct the identification algorithm. In particular, these theorems manage to convexify several non-convex constraints in general, so our proposed method can solve the problem efficiently. Details are explained in the following subsections.

2.3.1 Sparsity Invariance Theorem

The Sparsity Invariance (SI) theorem[11] was initially introduced and utilized to convexify the design of a controller to optimize the system's closed-loop behavior, subject to some specific sparsity constraints on the fractional structure of the controller. More specifically, the author suggests designing sparsity patterns for transfer matrices $\mathbf{D}(z)$ and $\mathbf{N}(z)$ such that the controller $\mathbf{K} = \mathbf{D}(z)^{-1}\mathbf{N}(z)$ demonstrates the desired sparsity architecture. This novel idea, however, is not restricted to controller design; as motivated by the duality of identification and control, we can also apply it to constrain the sparsity structure of the estimated system.

The main contribution of the SI concept can be summarized as an algorithm and a theorem. Given any binary matrix $S \in \{0,1\}^{n_y \times n_u}$, a binary matrix R_S^* can be uniquely generated via Algorithm 1 with a complexity of $\mathcal{O}(n_u \cdot n_y^2)$.

Algorithm 1 Generation of R_S^*

```
Input S ∈ {0,1}^{n_y × n_u}
Initialize R_S^* = 𝟙^{n_y × n_y}
for i = 1 : n_u and j = 1 : n_y do
    if S(j,i) == 0 then
        for k = 1 : n_y do
            if S(k,i) == 1 then
                R_S^*(j,k) = 0
            end if
        end for
    end if
end for
Return R_S^*
```

Theorem 1. ***Sparsity Invariance Theorem****[11]*
Let $S \in \{0,1\}^{n_y \times n_u}$ be any binary matrix and $R = R_S^* \in \{0,1\}^{n_y \times n_y}$ generated by Algorithm 1. Then,

- $\forall\ \mathbf{A} \in \text{Sparse}(R)$, $\mathbf{A}$ invertible and $\mathbf{B} \in \text{Sparse}(S)$, $\mathbf{A}^{-1}\mathbf{B} \in \text{Sparse}(S)$
- $\exists\ \mathbf{A}$ and $\mathbf{B}$ where $\text{Struct}(\mathbf{A}) = R$, $\mathbf{A}$ invertible and $\text{Struct}(\mathbf{B}) = S$ s.t. $\text{Struct}(\mathbf{A}^{-1}\mathbf{B}) = S$

Therefore, for all system identification problems involving fractional representation $\mathbf{G} = \mathbf{A}^{-1}\mathbf{B}$, the SI theorem replaces the generally non-convex constraint $\mathbf{G} \in \text{Sparse}(S)$ with convex constraints $\mathbf{A} \in \text{Sparse}(R)$ and $\mathbf{B} \in \text{Sparse}(S)$, and further proves that the resultant estimate of $\mathbf{G}$ is guaranteed to have the desired sparsity structure. The theorem is used to generate the sparsity constraints during optimization, as discussed in the next chapter.

2.3.2 Gershgorin Circle Theorem

The Gershgorin circle theorem[13] has been frequently used to analyze the spectrum of a square complex matrix, and the theorem is given below.

Theorem 2. ***Gershgorin Circle Theorem****[13]*
For any square complex matrix $A \in \mathbb{C}^{n \times n}$ with each (i, j)-entry $a_{ij} \in \mathbb{C}$,

$$\text{Spec}(A) \subset \bigcup_{i=1,\cdots,n} \left\{ z \in \mathbb{C} \mid \|z - a_{ii}\|_{\mathbb{C}} \leqslant \sum_{j=1, j\neq i}^{n} |a_{ij}| \right\}$$

This theorem indicates if the main diagonals dominate the norm of a matrix, the eigenvalues of the matrix are located in the proximity of the main diagonals. A typical application of Theorem 2 is to sufficiently ensure the invertibility of a matrix using a group of linear inequality constraints as given in the following corollary.

Corollary 1. *Suppose a square complex matrix $A \in \mathbb{C}^{n\times n}$ has (i, j)-entries $a_{ij} \in \mathbb{C}$, then*

$$|a_{ii}| > \sum_{j=1, j\neq i}^{n} |a_{ij}| \;\Rightarrow\; \text{A is invertible.}$$

This corollary is helpful and will be further discussed in Section 3.2.2 to ensure the stable invertibility of a transfer matrix. We will also provide a relaxation of these constraints in case they are too conservative.

Chapter 3

The Dual-Youla Parameterization

In this Chapter, we will focus on the dual-Youla identification method, which relies on the fractional representation[9] of the plant and has been extensively applied in system modeling and control synthesis[14]. The main advantage of the dual-Youla method is that the estimated plant is guaranteed to be stabilized by the given controller, which is crucial if the true plant is unstable. In this case, a good approximation of the closed-loop behavior is obviously more of interest than the open-loop behavior, especially when the estimate is intended for model-based controllers[15]. Considering the fact that large-scale systems can usually suffer from instability, the dual-Youla parameterization outperforms its competitors in identifying intrinsically unstable systems and is worth investigating.

In Section 3.1, we first explain how the original dual-Youla method identifies a general plant, followed by Section 3.2, which introduces the extended dual-Youla method equipped with sparsity constraints. Finally, Section 3.3 describes the extended method's implementation and the closed-form solutions' calculation.

3.1 Fundamentals of Dual-Youla Method

The dual-Youla method considers a simplified system model as follows,

$$\begin{aligned} y(k) &= \mathbf{G}(z)u(k) + \mathbf{H}(z)e(k) \\ u(k) &= \mathbf{K}(z)y(k) + r(k) \end{aligned} \tag{3.1}$$

The excitation signal $r(k)$ provides a reference for the control input $u(k)$. The noise $e(k)$ is defined as a sequence of correlated output errors and has the same dimension as $y(k)$. In this case, the noise dynamics $\mathbf{H}$ is assumed to be square, invertible, and exhibit a moving average (MA) structure.

The underlying idea of the conventional dual-Youla method is providing a parameterization of all plants $\mathbf{G}$ stabilized by a fixed positive feedback controller $\mathbf{K}$. Suppose the controller admits coprime factorization[16] such that $\mathbf{K} = \mathbf{D}_K^{-1}\mathbf{N}_K$ where $\mathbf{D}_K$ and $\mathbf{N}_K$ form a pair of stable and causal left coprime factors (no common unstable zeros). Further let $\mathbf{G}_X = \mathbf{D}_X^{-1}\mathbf{N}_X$ be any coprime-factorizable plant stabilized by $\mathbf{K}$. Then, the following set

$$\mathcal{G} = \left\{ \mathbf{G}(z,\theta) := \left(\mathbf{D}_X(z) + \mathbf{Q}(z,\theta)\mathbf{N}_K(z)\right)^{-1} \left(\mathbf{N}_X(z) + \mathbf{Q}(z,\theta)\mathbf{D}_K(z)\right) \mid \mathbf{Q}(z,\theta) \in \mathcal{RH}_\infty \right\}$$

includes all systems stabilized by $\mathbf{K}$ as a function of the so-called Youla parameter $\mathbf{Q}(\theta)$, which is stable, causal, and parameterized by a set of parameters θ. The true Youla parameter $\mathbf{Q}_0$ can

be uniquely determined in terms of the true plant $\mathbf{G}_0$ as follows,

$$\mathbf{Q}_0 = (\mathbf{D}_X\mathbf{G}_0 - \mathbf{N}_X) \cdot (\mathbf{D}_K - \mathbf{N}_K\mathbf{G}_0)^{-1} \tag{3.2}$$

We can then rewrite the input-output dynamics as follows,

$$\begin{aligned} & y(k) = \mathbf{G}u(k) + \mathbf{H}e(k) = (\mathbf{D}_X + \mathbf{Q}\mathbf{N}_K)^{-1}(\mathbf{N}_X + \mathbf{Q}\mathbf{D}_K)\,u(k) + \mathbf{H}e(k) \\ \Rightarrow\ & (\mathbf{D}_X + \mathbf{Q}\mathbf{N}_K)\,y(k) = (\mathbf{N}_X + \mathbf{Q}\mathbf{D}_K)\,u(k) + (\mathbf{D}_X + \mathbf{Q}\mathbf{N}_K)\,\mathbf{H}e(k) \\ \Rightarrow\ & (\mathbf{D}_X y(k) - \mathbf{N}_X u(k)) = \mathbf{Q}\,(\mathbf{D}_K u(k) - \mathbf{N}_K y(k)) + (\mathbf{D}_X + \mathbf{Q}\mathbf{N}_K)\,\mathbf{H}e(k) \\ \Rightarrow\ & \beta(k) = \mathbf{Q}\alpha(k) + \mathbf{L}e(k) \end{aligned} \tag{3.3}$$

Here, the filtered signal $\alpha(k) = \mathbf{D}_K u(k) - \mathbf{N}_K y(k) = \mathbf{D}_K r(k)$ only relates to the excitation $r(k)$ thus independent of both $\beta(k)$ and $e(k)$. This means the original closed-loop system is equivalent to another open-loop system with $\beta(k)$ and $\alpha(k)$ being its output and input signals. Hence, the dual-Youla method suggests computing an estimate of a stable and causal $\hat{\mathbf{Q}}$ of $\mathbf{Q}_0$ in an open-loop setup, instead of identifying $\mathbf{G}_0$ using the closed-loop data. Eventually, the estimate $\hat{\mathbf{G}}$ of the true plant $\mathbf{G}_0$ is given by

$$\hat{\mathbf{G}} = \left(\mathbf{D}_X + \hat{\mathbf{Q}}\mathbf{N}_K\right)^{-1}\left(\mathbf{N}_X + \hat{\mathbf{Q}}\mathbf{D}_K\right) \tag{3.4}$$

And the stabilizability of $\hat{\mathbf{G}}$ can be easily proved by computing the closed-loop transfer functions, i.e. $\left(I - \hat{\mathbf{G}}\mathbf{K}_0\right)^{-1}$ and $\left(I - \hat{\mathbf{G}}\mathbf{K}_0\right)^{-1}\hat{\mathbf{G}}$.

3.2 Methodologies

This section starts with elaborating on the extension of the conventional dual-Youla method with the Sparsity Invariance Theorem[11]. Subsequently, we define the Stable Invertibility Theorem, which we propose and prove with the purpose of ensuring the modified expression of the plant estimate $\hat{\mathbf{G}}$ consists of two coprime factors, thus guaranteeing the known controller stabilizes it.

3.2.1 Extended Dual-Youla Method

This section will introduce how to adapt the sparsity constraints to the original dual-Youla method. Suppose we want to estimate $\mathbf{G}_0 \in \text{Sparse}(S)$ and already obtain the binary matrix R w.r.t. S via Algorithm 1. Given an arbitrary guess of the plant $\mathbf{G}_X$ and an exactly known controller $\mathbf{K}_0$, we consider several extra assumptions in addition to the general assumptions defined in Section 2.1 ensure the functionality of our proposed method:

1). Both $\mathbf{G}_X$ and $\mathbf{G}_0$ are stabilizable and detectable, and in particular, stabilized by $\mathbf{K}_0$.

2). $\mathbf{G}_0$, $\mathbf{G}_X$ and $\mathbf{K}_0$ are coprime factorizable.

3). There exist FIR coprime factors $(\mathbf{D}_X, \mathbf{N}_X)$ for $\mathbf{G}_X$, $(\mathbf{D}_K, \mathbf{N}_K)$ for $\mathbf{K}_0$, and additionally $\mathbf{D}_X \in \text{Sparse}(R)$, $\mathbf{N}_X \in \text{Sparse}(S)$.

4). There exists a pair of coprime factors $(\mathbf{A}_{Q,0}, \mathbf{B}_{Q,0})$ s.t.

   i). $\mathbf{Q}_0 = \mathbf{A}_{Q,0}^{-1}\mathbf{B}_{Q,0}$

   ii). $\mathbf{A}_{Q,0}$ is stably invertible

   iii). $\text{Struct}\,(\mathbf{A}_{Q,0}\mathbf{D}_X + \mathbf{B}_{Q,0}\mathbf{N}_K) = R$

   iv). $\text{Struct}\,(\mathbf{A}_{Q,0}\mathbf{N}_X + \mathbf{B}_{Q,0}\mathbf{D}_K) = S$

Where the true Youla parameter $\mathbf{Q}_0$ has been defined in Eq.3.2. Assumptions 1). and 2). guarantee the estimate $\hat{\mathbf{G}}$ is stabilized by $\mathbf{K}_0$. Assumption 3). indicates $\mathbf{G}_X$ has the same or sparser structure than $\mathbf{G}_0$, and the factors have FIR representations with a common[1] FIR length of τ. Eq.3.5 shows an example of an FIR factor.

$$\mathbf{D}_X(z) = D_X^0 + D_X^1 \cdot z^{-1} + \cdots + D_X^{\tau-1} \cdot z^{-(\tau-1)} \tag{3.5}$$

Please note the index k is different in D_X^k and z^{-k}; D_X^k is a real matrix and stands for the k-th tap of $\mathbf{D}_X$, while z^{-k} means the k-th power of the shift operator z^{-1} $\forall k = 0, \cdots, \tau - 1$. We can also define the FIR representations for $\mathbf{N}_X$, $\mathbf{D}_K$ and $\mathbf{N}_K$ similar to Eq.3.5, which are then used to generate sparsity constraints as discussed in the next paragraph. With these three additional assumptions, we can already construct the following constrained optimization problem,

$$\begin{aligned} \min_{\mathbf{Q}\in\mathcal{RH}_\infty} \quad & \|\beta(k) - \mathbf{Q}\alpha(k)\| \\ \text{s.t. } & \mathbf{D}_X + \mathbf{Q}\mathbf{N}_K \in \text{Sparse}(R) \\ & \mathbf{N}_X + \mathbf{Q}\mathbf{D}_K \in \text{Sparse}(S) \end{aligned} \tag{3.6}$$

By parameterizing $\mathbf{Q}$ with FIR. Problem 3.6 then consists of a quadratic cost function that minimizes the model fitting error as explained in section, and a group of sparsity constraints that ensure $\hat{\mathbf{G}} \in \text{Sparse}(S)$, according to the SI theorem[11]. These sparsity constraints, under Assumption 3)., are defined as follows,

$$\begin{aligned} & \mathbf{D}_X + \mathbf{Q}\mathbf{N}_K \in \text{Sparse}(R) \\ & \qquad \Downarrow \\ & \text{Struct}(D_X^0 + Q^0 \cdot N_K^0) = R \\ & \text{Struct}(D_X^1 + Q^0 \cdot N_K^1 + Q^1 \cdot N_K^0) = R \\ & \text{Struct}(D_X^2 + Q^0 \cdot N_K^2 + Q^1 \cdot N_K^1 + Q^2 \cdot N_K^0) = R \\ & \qquad \vdots \end{aligned} \tag{3.7}$$

As $Q^i \cdot N_K^j$ represents the $(i+j)$-th tap of the matrix polynomial that is computed via the convolution of $\mathbf{Q}$ and $\mathbf{N}_K$, and similar for $\mathbf{N}_X + \mathbf{Q}\mathbf{D}_K \in \text{Sparse}(S)$. These linear equality constraints are implementable and still preserve the convexity of the optimization problem. We are now able to obtain an estimate $\hat{\mathbf{Q}}_N$ via Problem 3.6 before computing $\hat{\mathbf{G}}_N$ via Eq.3.4, provided a sequence of data with length N. However, a necessary condition of consistent $\hat{\mathbf{G}}_N$ is that the sparsity constraints are true for $\mathbf{Q}_0$, i.e.,

$$\lim_{N\to\infty} \hat{\mathbf{G}}_N \to \mathbf{G}_0 \quad \text{ only if } \quad \begin{aligned} & \mathbf{D}_X + \mathbf{Q}_0\mathbf{N}_K \in \text{Sparse}(R) \\ & \mathbf{N}_X + \mathbf{Q}_0\mathbf{D}_K \in \text{Sparse}(S) \end{aligned} \tag{3.8}$$

Which are generally impossible since $\text{Struct}(\mathbf{Q}_0) \geqslant \text{Struct}(\mathbf{G}_0) = S$ and $\text{Struct}(\mathbf{D}_K) \geqslant I_{n_u}$. Therefore, we introduce a so-called Sparsity Filter $\mathbf{A}_{Q,0}$ and define $\mathbf{B}_{Q,0} = \mathbf{A}_{Q,0} \cdot \mathbf{Q}_0$. Clearly, $\mathbf{A}_{Q,0}$ does not influence the resultant estimate since,

$$\begin{aligned} & \left(\mathbf{A}_{Q,0}\mathbf{D}_X + \mathbf{B}_{Q,0}\mathbf{N}_K\right)^{-1} \left(\mathbf{A}_{Q,0}\mathbf{N}_X + \mathbf{B}_{Q,0}\mathbf{D}_K\right) \\ = & \left(\mathbf{D}_X + \mathbf{Q}_0\mathbf{N}_K\right)^{-1} \mathbf{A}_{Q,0}^{-1}\mathbf{A}_{Q,0}(\mathbf{N}_X + \mathbf{Q}_0\mathbf{D}_K) \\ = & \left(\mathbf{D}_X + \mathbf{Q}_0\mathbf{N}_K\right)^{-1} \left(\mathbf{N}_X + \mathbf{Q}_0\mathbf{D}_K\right) = \mathbf{G}_0 \end{aligned} \tag{3.9}$$

[1] In real case, $\mathbf{D}_X$, $\mathbf{N}_X$, $\mathbf{D}_K$ and $\mathbf{N}_K$ do not necessarily have a common FIR length; we can consider augmenting them with transfer matrices of zeros as if they have the same length.

If $\mathbf{A}_{Q,0}$ is stably invertible[2]. It means $\mathbf{A}_{Q,0}$ has a stable and causal inverse, which a series of linear constraints can guarantee according to the Stable Invertibility Theorem in Section 3.2.2. Correspondingly, we introduce Assumption 4)., which indicates an equivalent ARX representation of $\mathbf{Q}_0$ and ensures $\mathbf{G}_0$ lies in the candidate set of estimates, as a necessary condition of unbiasedness and consistency. The idea behind the ARX representation is that $\mathbf{A}_{Q,0}$ projects the coprime factors in Eq.3.8 onto Sparse(R) and Sparse(S) respectively, so that the second statement of the Sparsity Invariance Theorem is effective. Note that $\mathbf{A}_{Q,0}$ is not unique; we can always multiply $\mathbf{A}_{Q,0}$ with another stably invertible transfer matrix without violating Eq.3.9. Therefore, the identification problem is now equivalent to solving the following optimization problem,

$$\begin{aligned} \min_{\mathbf{A}_Q,\, \mathbf{B}_Q \in \mathcal{RH}_\infty} \quad & \|\mathbf{A}_Q \beta(k) - \mathbf{B}_Q \alpha(k)\| \\ \text{s.t. } & \mathbf{A}_Q \mathbf{D}_X + \mathbf{B}_Q \mathbf{N}_K \in \text{Sparse}(R) \\ & \mathbf{A}_Q \mathbf{N}_X + \mathbf{B}_Q \mathbf{D}_K \in \text{Sparse}(S) \\ & \mathbf{A}_Q \text{ is stably invertible} \end{aligned} \tag{3.10}$$

Which will be reformulated into a standard quadratic program in terms of vector variables in Section 3.3.

3.2.2 Stable Invertibility Theorem

The proposed Stable Invertibility is to figure out a set of conditions to ensure the stable invertibility of a square transfer matrix $\mathbf{A}(z) \in \mathcal{F}_\tau$. Stable invertibility can be critical in both theory and implementation. As will be discussed in Chapter 3, where we introduce the extended dual-Youla method, two coprime factors multiplying a stably invertible filter are still coprime, which is a necessary condition for the stabilizability of the estimated plant. However, in general, the sufficient and necessary conditions on stably invertible $\mathbf{A}(z)$ are non-convex and thus inefficient to be implemented in the algorithm. In this report, we instead propose a set of convex constraints on $\mathbf{A}(z)$ so that stable invertibility is sufficiently guaranteed. These constraints, however, are expected to conservatively restrict the optimal solution of $\mathbf{A}(z)$. Relaxation of the constraints and quantification of shrinkage of the feasible region are of interest, but out of the scope of this report.

Theorem 3. ***Stable Invertibility Theorem***
Suppose a square FIR transfer matrix $\mathbf{A}(z) \in \mathcal{F}_\tau^{n\times n}$ has the following representation,

$$\mathbf{A}(z) = A^0 + A^1 \cdot z^{-1} + \cdots + A^{\tau-1} \cdot z^{-(\tau-1)} \tag{3.11}$$

Where $A^k \in \mathbb{R}^{n\times n}$ stands for the k-th tap of $\mathbf{A}(z)$ $\forall k = 0, \cdots, \tau-1$.
Then, given any arbitrary constant $c_0 \in \mathbb{R}_+$, $\mathbf{A}(z)$ has a stable and causal inverse if the following conditions are satisfied $\forall\, i = 1, \cdots, n$,

$$A^0_{ii} \geqslant c_0 \tag{3.12}$$

$$\sum_{k=1}^{\tau-1} \left|A^k_{ii}\right| + \sum_{k=0}^{\tau-1} \sum_{j=1, j\neq i}^{n} \left|A^k_{ij}\right| < c_0 \tag{3.13}$$

With A^k_{ij} representing the (i,j)-entry of A^k.

We first prove these constraints guarantee the existence of a stable and causal inverse of $\mathbf{A}(z)$, by showing $\mathbf{A}(z)$ has only asymptotically stable transmission zeros, i.e., having full rank $\forall\, |z| \geqslant 1$.

[2]Any invertible $\mathbf{A}_{Q,0}$ suffices Eq.3.9; we additionally need stable invertibility to ensure new factors are coprime.

Proof. Suppose $\mathbf{A}(z) \in \mathcal{F}_\tau^{n\times n}$ has the following form,

$$\mathbf{A}(z) = \begin{bmatrix} A_{11}(z) & A_{12}(z) & \cdots & A_{1n}(z) \\ A_{21}(z) & A_{22}(z) & \cdots & A_{2n}(z) \\ \vdots & \vdots & \ddots & \vdots \\ A_{n1}(z) & A_{n2}(z) & \cdots & A_{nn}(z) \end{bmatrix} = A^0 + A^1 \cdot z^{-1} + \cdots + A^{\tau-1} \cdot z^{-(\tau-1)} \tag{3.14}$$

Where $A_{ij}(z) \in \mathcal{F}_\tau$ is defined as,

$$A_{ij}(z) = a_{ij}^0 + a_{ij}^1 \cdot z^{-1} + \cdots + a_{ij}^{\tau-1} \cdot z^{-(\tau-1)}, \;\; a_{ij}^k \in \mathbb{R} \; \forall \; k = 0, \cdots, \tau - 1 \tag{3.15}$$

And A^k is identical to the definition in Eq.3.11. By Gershgorin Circle theorem, the complex square matrix $\mathbf{A}(z)$ has full rank if the following conditions hold:

$$|A_{ii}(z)| > \sum_{j=1, j\neq i}^{n} |A_{ij}(z)| \;\; \forall \text{ row } i \tag{3.16}$$

Then, expanding all the main diagonals of $\mathbf{A}(z)$ gives,

$$\begin{aligned} |A_{ii}(z)| &= \left|a_{ii}^0 + a_{ii}^1 z^{-1} + \cdots + a_{ii}^{\tau-1} z^{-(\tau-1)}\right| \\ &\geqslant \left|a_{ii}^0\right| - \left|a_{ii}^1 z^{-1}\right| - \cdots - \left|a_{ii}^{\tau-1} z^{-(\tau-1)}\right| \\ &\geqslant c_0 - \left|a_{ii}^1\right| \cdot \left|z^{-1}\right| - \cdots - \left|a_{ii}^{\tau-1}\right| \cdot \left|z^{-(\tau-1)}\right| \\ &\geqslant c_0 - \left|a_{ii}^1\right| - \cdots - \left|a_{ii}^{\tau-1}\right| \quad \forall \; |z| \geqslant 1 \\ &= c_0 - \sum_{k=1}^{\tau-1} \left|a_{ii}^k\right| \end{aligned} \tag{3.17}$$

Similarly, expanding all the off-diagonal terms leads to,

$$\begin{aligned} |A_{ij}(z)| &= \left|a_{ij}^0 + a_{ij}^1 z^{-1} + \cdots + a_{ij}^{\tau-1} z^{-(\tau-1)}\right| \\ &\leqslant \left|a_{ij}^0\right| + \left|a_{ij}^1 z^{-1}\right| + \cdots + \left|a_{ij}^{\tau-1} z^{-(\tau-1)}\right| \\ &\leqslant \left|a_{ij}^0\right| + \left|a_{ij}^1\right| \cdot \left|z^{-1}\right| + \cdots + \left|a_{ij}^{\tau-1}\right| \cdot \left|z^{-(\tau-1)}\right| \\ &\leqslant \left|a_{ij}^0\right| + \left|a_{ij}^1\right| + \cdots + \left|a_{ij}^{\tau-1}\right| \quad \forall \; |z| \geqslant 1 \\ &= \sum_{k=0}^{\tau-1} \left|a_{ij}^k\right| \end{aligned} \tag{3.18}$$

Therefore, Eq.3.16 can be implied by

$$|A_{ii}(z)| \geqslant c_0 - \sum_{k=1}^{\tau-1} \left|a_{ii}^k\right| > \sum_{j=1, j\neq i}^{n} \sum_{k=0}^{\tau-1} \left|a_{ij}^k\right| \geqslant \sum_{k=0}^{\tau-1} \sum_{j=1, j\neq i}^{n} \left|a_{ij}^k\right| \quad \forall \; i \tag{3.19}$$

In other words, Eq.3.12 and Eq.3.13 together imply Eq.3.16. Hence, by Gershgorin Circle Theorem, the spectrum of $\mathbf{A}(z)$ does not include the origin of the complex plane for all $|z| \geqslant 1$, implying $\mathbf{A}(z)$ has all zeros located on the open unit disk. Since $\mathbf{A}(z)$ is a causal square transfer matrix by construction, its number of poles equals the number of zeros and zeros of $\mathbf{A}(z)$ are identical to the poles of $\mathbf{A}(z)^{-1}$. Moreover, the DC tap A^0 is implicitly guaranteed to be invertible since $\mathbf{A}(z) \to A^0$ as $|z| \to \infty$, which correspondingly guarantees causal $\mathbf{A}(z)^{-1}$. Based on these properties, we conclude the solution of $\mathbf{A}(z)$ satisfying these constraints admits a stable and cause inverse. □

3.3 Implementation

This section explains how to efficiently solve Problem 3.10 and compute closed-form solutions of $\mathbf{A}_Q$ and $\mathbf{B}_Q$, by reformulating the cost function and constraints into quadratic and linear forms respectively. Specifically, we will first consider solving the problem via least squares (LS) before sequentially adding the sparsity constraints and stability invertibility conditions. In the last subsection, the instrumental variables (IV) method is also introduced in case the LS estimate is inconsistent.

3.3.1 Unconstrained Least Squares

We first consider the following FIR parameterizations with the time length $\tau \in \mathbb{R}$ as a hyperparameter[3],

$$\begin{aligned} \mathbf{A}_Q(z) &= I_{n_y} + A_Q^1 \cdot z^{-1} + \cdots + A_Q^{\tau-1} \cdot z^{-(\tau-1)} = I_{n_y} + z^{-1} \cdot \mathbf{A}_Q^*(z) \\ \mathbf{B}_Q(z) &= B_Q^0 + B_Q^1 \cdot z^{-1} + \cdots + B_Q^{\tau-1} \cdot z^{-(\tau-1)} \end{aligned} \tag{3.20}$$

Where the real matrices $A_Q^k \in \mathbb{R}^{n_y \times n_y}\ \forall k = 1, \cdots, \tau-1$ and $B_Q^k \in \mathbb{R}^{n_y \times n_u}\ \forall k = 0, \cdots, \tau-1$ are matrix variables to be determined. Correspondingly, the model fitting error $\epsilon(k) \in \mathbb{R}^{n_y}$ is expressed as,

$$\begin{aligned} \epsilon(k) &= \mathbf{A}_Q \beta(k) - \mathbf{B}_Q \alpha(k) \\ &= \beta(k) + \mathbf{A}_Q^* \cdot z^{-1} \beta(k) + \mathbf{B}_Q \alpha(k) \\ &= \beta(k) - \left(-\mathbf{A}_Q^* \beta(k-1) + \mathbf{B}_Q \alpha(k) \right) \\ &= \beta(k) - \Phi(k)^\top \cdot \theta \end{aligned} \tag{3.21}$$

Where the the vectorized variables θ and the regressor $\Phi(k)$ are defined as,

$$\theta = \begin{bmatrix} \theta_A \\ \theta_B \end{bmatrix} = \begin{bmatrix} \mathbf{vec}\left(\begin{bmatrix} A_Q^1 & A_Q^2 & \cdots & A_Q^{\tau-1} \end{bmatrix}^\top \right) \\ \mathbf{vec}\left(\begin{bmatrix} B_Q^0 & B_Q^1 & \cdots & B_Q^{\tau-1} \end{bmatrix}^\top \right) \end{bmatrix} \in \mathbb{R}^{n_\theta} \tag{3.22}$$

$$\Phi(k) = \begin{bmatrix} -I_{n_y} \bigotimes \begin{bmatrix} \beta(k-1) \\ \beta(k-2) \\ \vdots \\ \beta(k-\tau+1) \end{bmatrix} \\ I_{n_y} \bigotimes \begin{bmatrix} \alpha(k) \\ \alpha(k-1) \\ \vdots \\ \alpha(k-\tau+1) \end{bmatrix} \end{bmatrix} \in \mathbb{R}^{n_\theta \times n_y} \tag{3.23}$$

With $n_\theta = (\tau-1) \cdot n_y^2 + \tau \cdot n_y n_u$ representing the total number of variables to be estimated. By stacking $\beta(k)$ and $\Phi(k)^\top\ \forall k = 0, \cdots, N-1$,

$$\boldsymbol{\beta} = \begin{bmatrix} \beta(0) \\ \beta(1) \\ \vdots \\ \beta(N-1) \end{bmatrix} \in \mathbb{R}^{N \cdot n_y} \quad \boldsymbol{\Phi} = \begin{bmatrix} \Phi(0)^\top \\ \Phi(1)^\top \\ \vdots \\ \Phi(N-1)^\top \end{bmatrix} \in \mathbb{R}^{(N \cdot n_y) \times n_\theta} \tag{3.24}$$

[3]The FIR length of $\mathbf{A}_Q$ and $\mathbf{B}_Q$ can be chosen differently based on the a-priori knowledge of the order of $\mathbf{G}_0$.

We can compute the (unconstrained) Least Squares (LS) solution,

$$\hat{\theta}_N^{LS} = \underset{\theta}{\operatorname{argmin}} \ \|\boldsymbol{\beta} - \boldsymbol{\Phi}\theta\|_2 = \left(\boldsymbol{\Phi}^\top \boldsymbol{\Phi}\right)^{-1} \boldsymbol{\Phi}^\top \boldsymbol{\beta} \tag{3.25}$$

Which provides a rough estimate $\mathbf{Q}^{LS}$ without utilizing the knowledge of sparsity structures.

3.3.2 Constrained Least Squares

Moving on, we can expand the sparsity constraints $\mathbf{A}_Q\mathbf{D}_X + \mathbf{B}_Q\mathbf{N}_K \in \text{Sparse}(R)$ as below,

$$\begin{aligned}
&\begin{bmatrix} I_{n_y} & A_Q^1 & \cdots & A_Q^{\tau-1} \end{bmatrix} \begin{bmatrix} D_X^0 & D_X^1 & \cdots & D_X^{\tau-1} & \mathbf{0} & \cdots & \mathbf{0} \\ \mathbf{0} & D_X^0 & \cdots & D_X^{\tau-2} & D_X^{\tau-1} & \cdots & \mathbf{0} \\ \vdots & \vdots & \ddots & \vdots & \vdots & \ddots & \vdots \\ \mathbf{0} & \mathbf{0} & \cdots & D_X^0 & D_X^1 & \cdots & D_X^{\tau-1} \end{bmatrix} \\
&+ \begin{bmatrix} B_Q^0 & B_Q^1 & \cdots & B_Q^{\tau-1} \end{bmatrix} \begin{bmatrix} N_K^0 & N_K^1 & \cdots & N_K^{\tau-1} & \mathbf{0} & \cdots & \mathbf{0} \\ \mathbf{0} & N_K^0 & \cdots & N_K^{\tau-2} & N_K^{\tau-1} & \cdots & \mathbf{0} \\ \vdots & \vdots & \ddots & \vdots & \vdots & \ddots & \vdots \\ \mathbf{0} & \mathbf{0} & \cdots & N_K^0 & N_K^1 & \cdots & N_K^{\tau-1} \end{bmatrix} \\
&= \begin{bmatrix} I_{n_y} & A_Q^1 & \cdots & A_Q^{\tau-1} \end{bmatrix} \cdot \mathbf{toep}(\mathbf{D}_X, \tau) + \begin{bmatrix} B_Q^0 & B_Q^1 & \cdots & B_Q^{\tau-1} \end{bmatrix} \cdot \mathbf{toep}(\mathbf{N}_K, \tau) \\
&= \begin{bmatrix} D_X^0 & D_X^1 & \cdots & D_X^{\tau-1} & \mathbf{0} & \cdots & \mathbf{0} \end{bmatrix}^{\#} \\
&+ \begin{bmatrix} A_Q^1 & A_Q^2 & \cdots & A_Q^{\tau-1} \end{bmatrix} \cdot \mathbf{toep}(\mathbf{D}_X, \tau - 1) \\
&+ \begin{bmatrix} B_Q^0 & B_Q^1 & \cdots & B_Q^{\tau-1} \end{bmatrix} \cdot \mathbf{toep}(\mathbf{N}_K, \tau) \\
&\in \text{Sparse}\left(\begin{bmatrix} R & R & \cdots & R \end{bmatrix}\right)
\end{aligned} \tag{3.26}$$

With $\mathbf{toep}(\mathbf{A}, \nu)$ indicating the Toeplitz operation of an FIR transfer matrix $\mathbf{A}$ by repeating ν times. Because of Assumption 3). such that $\mathbf{D}_X \in \text{Sparse}(R)$, the expression $\#$ naturally satisfies the sparsity constraints, thus removing it has no impact on the resultant estimate. We then manage to rewrite the sparsity constraints into, We first construct a matrix $\tilde{\mathbf{E}}_R$ by,

$$\tilde{\mathbf{E}}_R = \left[I_{n_y} \bigotimes \mathbf{toep}(\mathbf{D}_X, \tau - 1)^\top, \ I_{n_y} \bigotimes \mathbf{toep}(\mathbf{N}_K, \tau)^\top\right] \tag{3.27}$$

Let us define $\mathbf{R} = [R, R, \cdots, R]$, hence the sparsity constraints are equivalent to,

$$\tilde{\mathbf{E}}_R \cdot \theta \in \text{Sparse}\left(\mathbf{vec}\left(\mathbf{R}^\top\right)\right) \tag{3.28}$$

We next construct the equality constraint matrix $\mathbf{E}_R$ associated with R, by removing the i-th row of $\tilde{\mathbf{E}}_R$ if the i-th element of $\mathbf{vec}\left(\mathbf{R}^\top\right)$ equals 1. In MATLAB, this can be implemented as,

$$\mathbf{E}_R = \tilde{\mathbf{E}}_R\left(\mathbf{vec}\left(\mathbf{R}^\top\right) == 0\right) \tag{3.29}$$

We now manage to rewrite the sparsity constraints $\mathbf{A}_Q\mathbf{D}_X + \mathbf{B}_Q\mathbf{N}_K \in \text{Sparse}(R)$ into $\mathbf{E}_R \cdot \theta = \mathbf{0}$. Similarly, we can construct $\mathbf{E}_S$ as follows,

$$\begin{aligned}
\tilde{\mathbf{E}}_S &= \left[I_{n_y} \bigotimes \mathbf{toep}(\mathbf{N}_X, \tau - 1)^\top, \ I_{n_y} \bigotimes \mathbf{toep}(\mathbf{D}_K, \tau)^\top\right] \\
\mathbf{S} &= \begin{bmatrix} S & S & \cdots & S \end{bmatrix} \\
\mathbf{E}_S &= \tilde{\mathbf{E}}_S\left(\mathbf{vec}\left(\mathbf{S}^\top\right) == 0\right)
\end{aligned} \tag{3.30}$$

And finally, we have,

$$\mathbf{E} = \begin{bmatrix} \mathbf{E}_R \\ \mathbf{E}_S \end{bmatrix} \quad \Rightarrow \quad \mathbf{E}\theta = \mathbf{0} \text{ represents all sparsity constraints.} \tag{3.31}$$

Thus, the corresponding Constrained Least Squares (CLS) problem is given by,

$$\begin{aligned} &\min_{\theta} \ \|\boldsymbol{\beta} - \boldsymbol{\Phi}\theta\|_2 \\ &\text{s.t. } \mathbf{E}\theta = \mathbf{0} \end{aligned} \tag{3.32}$$

The Lagrangian form of Problem 3.32 is then given by,

$$\begin{bmatrix} \boldsymbol{\Phi}^\top\boldsymbol{\Phi} & \mathbf{E}^\top \\ \mathbf{E} & \mathbf{0} \end{bmatrix} \begin{bmatrix} \theta \\ \mu \end{bmatrix} = \begin{bmatrix} \boldsymbol{\Phi}^\top\boldsymbol{\beta} \\ \mathbf{0} \end{bmatrix} \tag{3.33}$$

With μ the vector of Lagrangian multipliers associated with the sparsity constraints. Hence, we can compute the CLS[4] solution based on the Schur complement[17],

$$\begin{aligned} \hat{\theta}_N^{CLS} &= \left[\mathbf{P}^{-1} - \mathbf{P}^{-1}\mathbf{E}^\top\left(\mathbf{E}\mathbf{P}^{-1}\mathbf{E}^\top\right)^\dagger\mathbf{E}\mathbf{P}^{-1}\right]\boldsymbol{\Phi}^\top\boldsymbol{\beta} \\ &= \hat{\theta}_N^{LS} - \mathbf{P}^{-1}\mathbf{E}^\top\left(\mathbf{E}\mathbf{P}^{-1}\mathbf{E}^\top\right)^\dagger\mathbf{E}\cdot\hat{\theta}_N^{LS} \\ &= \text{LS Estimate} + \text{Sparsity Rejection} \end{aligned} \tag{3.34}$$

Where the Hessian matrix $\mathbf{P} = \boldsymbol{\Phi}^\top\boldsymbol{\Phi}$ is guaranteed to be invertible by the assumption of persistently exciting input signals. An interpretation of Eq.3.34 is that the sparsity constraints generate a rejection vector that is linear to $\hat{\theta}_N^{LS}$ and reject it into the sparsity space. Equivalently, we can define the rejection matrix

$$\boldsymbol{\Pi} = \mathbf{P}^{-1}\mathbf{E}^\top\left(\mathbf{E}\mathbf{P}^{-1}\mathbf{E}^\top\right)^\dagger\mathbf{E} \tag{3.35}$$

So that $\hat{\theta}_N^{CLS} = (I_{n_\theta} - \boldsymbol{\Pi})\hat{\theta}_N^{LS}$. Suppose the expectation of the LS estimate is given by $\mathbb{E}[\hat{\theta}_N^{LS}] = \bar{\theta}$. When the sparsity constraints are true for $\bar{\theta}$, i.e. $\mathbf{E}\cdot\bar{\theta} = \mathbf{0}$, we can prove $\hat{\theta}_N^{CLS}$ has exacly the same expectation and converges to $\bar{\theta}$ more efficiently than $\hat{\theta}_N^{LS}$, as shown below.

$$\begin{aligned} \mathbb{E}\left[\hat{\theta}_N^{CLS}\right] &= \mathbb{E}\left[\hat{\theta}_N^{LS}\right] - \mathbf{P}^{-1}\mathbf{E}^\top\left(\mathbf{E}\mathbf{P}^{-1}\mathbf{E}^\top\right)^\dagger\left(\mathbf{E}\cdot\mathbb{E}\left[\hat{\theta}_N^{LS}\right]\right) \\ &= \bar{\theta} - \mathbf{P}^{-1}\mathbf{E}^\top\left(\mathbf{E}\mathbf{P}^{-1}\mathbf{E}^\top\right)^\dagger\left(\mathbf{E}\cdot\bar{\theta}\right) = \bar{\theta} \end{aligned} \tag{3.36}$$

Meanwhile, the variance of $\hat{\theta}_N^{CLS}$ is,

$$\begin{aligned} \mathbf{Var}\left(\hat{\theta}_N^{CLS}\right) &= \mathbb{E}\left[\left(\hat{\theta}_N^{CLS} - \bar{\theta}\right)\left(\hat{\theta}_N^{CLS} - \bar{\theta}\right)^\top\right] \\ &= (I_{n_\theta} - \boldsymbol{\Pi})\cdot\mathbb{E}\left[\left(\hat{\theta}_N^{LS} - \bar{\theta}\right)\left(\hat{\theta}_N^{LS} - \bar{\theta}\right)^\top\right]\cdot(I_{n_\theta} - \boldsymbol{\Pi})^\top \\ &= \mathbf{Var}\left(\hat{\theta}_N^{LS}\right) + \boldsymbol{\Pi}\cdot\mathbf{Var}\left(\hat{\theta}_N^{LS}\right)\cdot\boldsymbol{\Pi}^\top - \boldsymbol{\Pi}\cdot\mathbf{Var}\left(\hat{\theta}_N^{LS}\right) - \mathbf{Var}\left(\hat{\theta}_N^{LS}\right)\cdot\boldsymbol{\Pi}^\top \end{aligned} \tag{3.37}$$

[4]The solution involves pseudo-inverse since $\mathbf{E}\left(\boldsymbol{\Phi}^T\boldsymbol{\Phi}\right)^{-1}\mathbf{E}^\top$ is always singular, in accordance with the fact that $\mathbf{A}_Q$ and $\mathbf{B}_Q$ are not unique.

Given $\mathbf{Var}(\hat{\theta}_N^{LS}) = \mathbf{P}^{-1}$, we have,

$$\begin{aligned}\mathbf{\Pi} \cdot \mathbf{Var}\left(\hat{\theta}_N^{LS}\right) \cdot \mathbf{\Pi}^\top &= \mathbf{P}^{-1}\mathbf{E}^\top \left(\mathbf{E}\mathbf{P}^{-1}\mathbf{E}^\top\right)^\dagger \mathbf{E} \cdot \mathbf{P}^{-1} \cdot \mathbf{E}^\top \left(\mathbf{E}\mathbf{P}^{-1}\mathbf{E}^\top\right)^\dagger \mathbf{E}\mathbf{P}^{-1} \\ &= \mathbf{P}^{-1}\mathbf{E}^\top \left(\mathbf{E}\mathbf{P}^{-1}\mathbf{E}^\top\right)^\dagger \mathbf{E} \cdot \mathbf{P}^{-1} \cdot \mathbf{E}^\top \left(\mathbf{E}^\top\right)^\dagger \left(\mathbf{E}\mathbf{P}^{-1}\right)^\dagger \mathbf{E}\mathbf{P}^{-1} \\ &= \mathbf{P}^{-1}\mathbf{E}^\top \left(\mathbf{E}\mathbf{P}^{-1}\mathbf{E}^\top\right)^\dagger \mathbf{E} \cdot \mathbf{P}^{-1}\end{aligned} \tag{3.38}$$

Therefore, combining Eq.3.37 and 3.38 results in,

$$\mathbf{Var}\left(\hat{\theta}_N^{CLS}\right) = \mathbf{Var}\left(\hat{\theta}_N^{LS}\right) - \mathbf{P}^{-1}\mathbf{E}^\top \left(\mathbf{E}\mathbf{P}^{-1}\mathbf{E}^\top\right)^\dagger \mathbf{E} \cdot \mathbf{P}^{-1} \tag{3.39}$$

Clearly, $\mathbf{P}^{-1}\mathbf{E}^\top \left(\mathbf{E}\mathbf{P}^{-1}\mathbf{E}^\top\right)^\dagger \mathbf{E} \cdot \mathbf{P}^{-1}$ is positive semi-definite, thus $\hat{\theta}_N^{CLS}$ in general has a smaller variance than $\hat{\theta}_N^{LS}$.

3.3.3 Regularized Constrained Least Squares

The CLS estimate is useful when we are lucky enough to have a stably invertible $\hat{\mathbf{A}}_Q^{CLS}$, since it preserves the property of being coprime for the new factors, but this is not always true. Hence, we need some additional constraints to enforce stable invertibility. By Theorem 3 explained in Section 3.2.2, the stable invertibility of $\mathbf{A}_Q$ is guaranteed if the following conditions based on Eq.3.13 are satisfied,

$$\sum_{k=1}^{\tau-1} \left|A_Q^k(i,i)\right| + \sum_{k=1}^{\tau-1} \sum_{j=1, j\neq i}^{n_y} \left|A_Q^k(i,j)\right| = \sum_{k=1}^{\tau-1} \sum_{j=1}^{n_y} \left|A_Q^k(i,j)\right| < 1 \;\; \forall i = 1, \cdots, n_y \tag{3.40}$$

Note $A_Q^0 = I_{n_y}$ hence Eq.3.12 (dominant main diagonals) is already fulfilled. Eq.3.40 can be further manipulated into an ℓ_1-norm constraint since,

$$\begin{gathered}\sum_{k=1}^{\tau-1} \sum_{i=1}^{n_y} \sum_{j=1}^{n_y} \left|A_Q^k(i,j)\right| \geqslant \sum_{k=1}^{\tau-1} \sum_{j=1}^{n_y} \left|A_Q^k(i,j)\right| \\ \Downarrow \\ \sum_{k=1}^{\tau-1} \sum_{i=1}^{n_y} \sum_{j=1}^{n_y} \left|A_Q^k(i,j)\right| = \|\theta_A\|_1 < 1 \quad \Rightarrow \quad \sum_{k=1}^{\tau-1} \sum_{j=1}^{n_y} \left|A_Q^k(i,j)\right| < 1 \; \forall i = 1, \cdots, n_y\end{gathered} \tag{3.41}$$

This implies, the stable invertibility of $\mathbf{A}_Q$ can be ensured by simply constraining $\|\theta_A\|_1$. Due to the equivalence of vector norms, i.e., $\|\theta_A\|_1 \leqslant \sqrt{(\tau-1)\cdot n_y^2} \cdot \|\theta_A\|_2$, we can replace the ℓ_1-norm constraint with an ℓ_2-norm constraint, which is more conservative but simpler to implement. Furthermore, the theory of LASSO[18] implies the ℓ_2-norm constraint can be further replaced with ℓ_2-norm regularization in the cost function without changing the optimal solution. Therefore, by considering the ℓ_2-norm regularization, the Regularized Constrained Least Squares (RCLS) problem is defined as,

$$\begin{gathered}\hat{\theta}_N^{RCLS}(\lambda) = \underset{\theta=[\theta_A^\top, \theta_B^\top]^\top}{\operatorname{argmin}} \; \frac{1}{2N} \|\boldsymbol{\beta} - \mathbf{\Phi}\theta\|_2^2 + \frac{\lambda}{2} \|\theta_A\|_2^2 \\ \text{s.t. } \mathbf{E}\theta = \mathbf{0}\end{gathered} \tag{3.42}$$

Where λ as a hyperparameter scales the penalty on $\|\theta_A\|_2$. Similar to Eq.3.34, the RCLS solution can be computed as,

$$\hat{\theta}_N^{RCLS} = \left[\mathbf{P}(\lambda)^{-1} - \mathbf{P}(\lambda)^{-1}\mathbf{E}^\top \left(\mathbf{E}\mathbf{P}(\lambda)^{-1}\mathbf{E}^\top\right)^\dagger \mathbf{E}\mathbf{P}(\lambda)^{-1}\right] \mathbf{\Phi}^\top \boldsymbol{\beta} \tag{3.43}$$

With a slightly different Hessian matrix $\mathbf{P}(\lambda)$ defined as,

$$\begin{aligned}\mathbf{P}(\lambda) &= \mathbf{\Phi}^\top \mathbf{\Phi} + N \cdot \mathbf{\Lambda}(\lambda) \\ \mathbf{\Lambda}(\lambda) &= \begin{bmatrix} \lambda \cdot I_{(\tau-1)\cdot n_y^2} & \mathbf{0} \\ \mathbf{0} & \mathbf{0} \end{bmatrix}\end{aligned} \tag{3.44}$$

The choice of λ influences the norm distribution of $\mathbf{A}_Q$: $\lambda = 0$ means there is no constraint at all, while by increasing λ to infinity, we shall expect $\mathbf{A}_Q$ approaches an identity matrix. The LASSO theory guarantees that there always exists a critical penalty constant λ_{crit} such that $\forall \lambda \geqslant \lambda_{crit}$, $\hat{\theta}_N^{RCLS}(\lambda)$ always satisfies the conditions in Eq.3.40 thus resulting in a stably invertible $\mathbf{A}_Q$. Note that regularization always leads to additional bias, which might be undesired in system identification. Hence, we suggest tuning λ from zero for the RCLS estimate, only if the CLS estimate loses stable invertibility.

3.3.4 Constrained Instrumental Variables

Previously, we discussed how to estimate the Youla parameter $\mathbf{Q}$ using least squares as if it has an ARX parameterization. In fact, the system dynamics involving output error is,

$$\begin{aligned} y(k) = \mathbf{G}u(k) + \mathbf{H}e(k) &\Rightarrow \mathbf{A}_Q(\theta)\beta(k) = \mathbf{B}_Q(\theta)\alpha(k) + \mathbf{L}_Q(\eta)e(k) \\ &\Rightarrow \beta(k) = \Phi(k)^\top \theta + v(k) \end{aligned} \tag{3.45}$$

Where $v(k) = \mathbf{L}_Q e(k) = \left(\mathbf{A}_Q \mathbf{D}_X + \mathbf{B}_Q \mathbf{N}_K\right) \mathbf{H} e(k)$ allows for an FIR parameterization[5] as well by construction. Therefore, the dynamics on the right side of Eq.3.45 exhibits an ARMAX structure, which means there exists a correlation between the regressor $\Phi(k)$ and noise $e(k)$, indicating the least squares method is not capable of an unbiased and consistent estimate[1]. Techniques tailored for an ARMAX model have been extensively investigated in the literature[19], yet the majority of these methods concentrate on SISO systems, making them not directly applicable in the presence of sparsity constraints. For this reason, we utilize the idea of instrumental variables[20] and introduce the Constrained Instrumental Variables (CIV) to eliminate the correlation. The approximated noise-free regressor at time k, denoted as $Z(k)$, has the same dimension as $\Phi(k)$ and must be uncorrelated with $v(k)$ but sufficiently correlated with $\Phi(k)$. More specifically,

$$\begin{aligned} &\mathbb{E}\left[Z(k)\Phi(k)^\top\right] \text{ is nonsingular} \\ &\mathbb{E}\left[Z(k)^\top v(k)\right] = 0 \end{aligned} \tag{3.46}$$

A common choice of instrument is the approximation of the noise-free regressor, by filtering the input signal ($\alpha(k)$ in this case) with a raw estimate of the system. Such a filter can be chosen as the LS estimate, which is generally applicable for a MIMO system[21]. Hence, we compute the instrument vector $\zeta(k)$ as an undisturbed approximation of $\beta(k)$ using the LS estimate[6],

$$\zeta(k) = \left(\hat{\mathbf{A}}_Q^{LS}\right)^{-1} \hat{\mathbf{B}}_Q^{LS} \cdot \beta(k) \tag{3.47}$$

[5] Eq.3.45 indicates $\mathbf{L}_Q$ can be parameterized independently denoted by η, as $\mathbf{H}$ is independent of $\mathbf{G}$.
[6] Sparsity constraints are not necessary for this step as we only need the filtered signal.

Then construct the instrument matrix,

$$Z(k) = \begin{bmatrix} -I_{n_y} \bigotimes \begin{bmatrix} \zeta(k-1) \\ \zeta(k-2) \\ \vdots \\ \zeta(k-\tau+1) \end{bmatrix} \\ I_{n_y} \bigotimes \begin{bmatrix} \alpha(k) \\ \alpha(k-1) \\ \vdots \\ \alpha(k-\tau+1) \end{bmatrix} \end{bmatrix} \tag{3.48}$$

Stacking $Z(k)$ for all $k = 0, \cdots, N$ gives,

$$\mathbf{Z} = \begin{bmatrix} Z(0)^\top \\ Z(1)^\top \\ \vdots \\ Z(N-1)^\top \end{bmatrix} \tag{3.49}$$

We first compute the unconstrained solution $\hat{\theta}_N^{IV}$ as follows,

$$\hat{\theta}_N^{IV} = \left(\mathbf{Z}^\top \mathbf{\Phi}\right)^{-1} \mathbf{Z}^\top \boldsymbol{\beta} \tag{3.50}$$

It is unbiased and consistent w.r.t. the true parameter θ_0 since $Z(k)$ is only dependent on α thus uncorrelated with $v(k)$, hence $\mathbb{E}[\hat{\theta}_N^{IV}] = \lim_{N\to\infty} \hat{\theta}_N^{IV} = \theta_0$. We further define $\hat{\theta}_N^{CIV}$ as the solution to the problem below,

$$\begin{aligned} &\mathbf{Z}^\top \mathbf{\Phi}\theta = \mathbf{Z}^\top \boldsymbol{\beta} \\ \text{s.t. } &\mathbf{E}\theta = \mathbf{0} \end{aligned} \tag{3.51}$$

Which, as we propose, can be solved via the following Lagrangian form,

$$\begin{bmatrix} \mathbf{Z}^\top \mathbf{\Phi} & \mathbf{E}^\top \\ \mathbf{E} & \mathbf{0} \end{bmatrix} \begin{bmatrix} \theta \\ \mu \end{bmatrix} = \begin{bmatrix} \mathbf{Z}^\top \boldsymbol{\beta} \\ \mathbf{0} \end{bmatrix} \tag{3.52}$$

$$\begin{aligned} \Rightarrow \hat{\theta}_N^{CIV} &= \left[\left(\mathbf{Z}^\top \mathbf{\Phi}\right)^{-1} - \left(\mathbf{Z}^\top \mathbf{\Phi}\right)^{-1} \mathbf{E}^\top \left(\mathbf{E}\left(\mathbf{Z}^\top \mathbf{\Phi}\right)^{-1} \mathbf{E}^\top\right)^\dagger \mathbf{E}\left(\mathbf{Z}^\top \mathbf{\Phi}\right)^{-1}\right] \mathbf{Z}^\top \boldsymbol{\beta} \\ &= \hat{\theta}_N^{IV} - \left(\mathbf{Z}^\top \mathbf{\Phi}\right)^{-1} \mathbf{E}^\top \left(\mathbf{E}\left(\mathbf{Z}^\top \mathbf{\Phi}\right)^{-1} \mathbf{E}^\top\right)^\dagger \mathbf{E} \cdot \hat{\theta}_N^{IV} \end{aligned} \tag{3.53}$$

We claim that $\hat{\theta}_N^{CIV}$ is also unbiased, consistent, and satisfies the sparsity constraints.

Proof. Given the IV estimate $\hat{\theta}_N^{IV}$ is unbiased and consistent, and sparsity constraints are true for θ_0, the CIV estimate $\hat{\theta}_N^{CIV}$ has:

1). **Unbiasedness.**

$$\begin{aligned} \mathbb{E}\left[\hat{\theta}_N^{CIV}\right] &= \mathbb{E}\left[\hat{\theta}_N^{IV}\right] - \left(\mathbf{Z}^\top \mathbf{\Phi}\right)^{-1} \mathbf{E}^\top \left(\mathbf{E}\left(\mathbf{Z}^\top \mathbf{\Phi}\right)^{-1} \mathbf{E}^\top\right)^\dagger \mathbf{E} \cdot \mathbb{E}\left[\hat{\theta}_N^{IV}\right] \\ &= \theta_0 - \left(\mathbf{Z}^\top \mathbf{\Phi}\right)^{-1} \mathbf{E}^\top \left(\mathbf{E}\left(\mathbf{Z}^\top \mathbf{\Phi}\right)^{-1} \mathbf{E}^\top\right)^\dagger \mathbf{E} \cdot \theta_0 = \theta_0 \end{aligned} \tag{3.54}$$

2). **Consistency.**

$$\begin{aligned}\lim_{N\to\infty}\hat{\theta}_N^{CIV} &= \lim_{N\to\infty}\hat{\theta}_N^{IV} - \left(\mathbf{Z}^\top\mathbf{\Phi}\right)^{-1}\mathbf{E}^\top\left(\mathbf{E}\left(\mathbf{Z}^\top\mathbf{\Phi}\right)^{-1}\mathbf{E}^\top\right)^\dagger\mathbf{E}\cdot\lim_{N\to\infty}\hat{\theta}_N^{IV}\\ &= \theta_0 - \left(\mathbf{Z}^\top\mathbf{\Phi}\right)^{-1}\mathbf{E}^\top\left(\mathbf{E}\left(\mathbf{Z}^\top\mathbf{\Phi}\right)^{-1}\mathbf{E}^\top\right)^\dagger\mathbf{E}\cdot\theta_0 = \theta_0\end{aligned} \tag{3.55}$$

3). **Sparsity constraints fulfilled.**

$$\begin{aligned}\mathbf{E}\hat{\theta}_N^{CIV} &= \mathbf{E}\hat{\theta}_N^{IV} - \mathbf{E}\left(\mathbf{Z}^\top\mathbf{\Phi}\right)^{-1}\mathbf{E}^\top\left(\mathbf{E}\left(\mathbf{Z}^\top\mathbf{\Phi}\right)^{-1}\mathbf{E}^\top\right)^\dagger\mathbf{E}\hat{\theta}_N^{IV}\\ &= \mathbf{E}\hat{\theta}_N^{IV} - \mathbf{E}\left(\mathbf{Z}^\top\mathbf{\Phi}\right)^{-1}\mathbf{E}^\top\left(\mathbf{E}\left(\mathbf{Z}^\top\mathbf{\Phi}\right)^{-1}\mathbf{E}^\top\right)^\dagger\mathbf{E}\left(\mathbf{Z}^\top\mathbf{\Phi}\right)^{-1}\mathbf{Z}^\top\boldsymbol{\beta}\\ &= \mathbf{E}\hat{\theta}_N^{IV} - \mathbf{E}\left(\mathbf{Z}^\top\mathbf{\Phi}\right)^{-1}\mathbf{E}^\top\left(\mathbf{E}^\top\right)^\dagger\left(\mathbf{E}\left(\mathbf{Z}^\top\mathbf{\Phi}\right)^{-1}\right)^\dagger\mathbf{E}\left(\mathbf{Z}^\top\mathbf{\Phi}\right)^{-1}\mathbf{Z}^\top\boldsymbol{\beta}\\ &= \mathbf{E}\hat{\theta}_N^{IV} - \mathbf{E}\left(\mathbf{Z}^\top\mathbf{\Phi}\right)^{-1}\cdot I\cdot I\cdot\mathbf{Z}^\top\boldsymbol{\beta} = \mathbf{0}\end{aligned} \tag{3.56}$$

□

Consequently, through the utilization of the IV method, we theoretically achieve an unbiased and consistent $\hat{\theta}_N^{CLS}$, resulting in an estimated plant $\hat{\mathbf{G}}_N^{CLS}$ that retains its unbiased and consistent attributes while conforming to the pre-defined sparsity pattern. Generally, the IV estimate becomes more desired when consistent estimation is of prime importance, though at the cost of increased computational complexity. However, in practical scenarios, consistency might not have priority; achieving an efficient approximation of the transfer function or output prediction could hold more significance. Thus, the choice between LS and IV hinges on the primary objective of the estimation. In Chapter 5, where we simulate an example system for verification purposes, we favor using the least-squares method. This preference is driven by the fact that the LS estimate already decently approximates the plant. Looking forward, the integration of the Sparsity Invariance Theorem into the IV method or other validated approaches tailored for the ARMAX structure could pave the way for future advancements.

Furthermore, it is important to acknowledge that the final estimate from the extended dual-Youla method might possess an unnecessarily high order. This occurs as a consequence of constructing both the denominator and numerator using the convolution of multiple FIR transfer matrices. Considering the expression of the true Youla parameter in Eq.3.2, we shall expect $\mathbf{Q}_0 = \mathbf{A}_{Q,0}^{-1}\mathbf{B}_{Q,0}$ has a higher order than the true model $\mathbf{G}_0 = \mathbf{D}_0^{-1}\mathbf{N}_0$. This implies, the estimate of the plant's factors,

$$\begin{aligned}\hat{\mathbf{D}}_Q &= \hat{\mathbf{A}}_Q\mathbf{D}_X + \hat{\mathbf{B}}_Q\mathbf{N}_K\\ \hat{\mathbf{N}}_Q &= \hat{\mathbf{A}}_Q\mathbf{N}_X + \hat{\mathbf{B}}_Q\mathbf{D}_K\end{aligned} \tag{3.57}$$

Have orders no shorter than $\mathbf{A}_{Q,0}$ or $\mathbf{B}_{Q,0}$, as a necessary condition to achieve an unbiased and consistent estimate $\hat{\mathbf{Q}} = \hat{\mathbf{A}}_Q^{-1}\hat{\mathbf{B}}_Q$. Thus, $\hat{\mathbf{D}}_Q$ generally has a larger order than $\mathbf{D}_0$ and same for $\hat{\mathbf{N}}_Q$, $\mathbf{N}_0$. Although established techniques for order reduction are available [22], it is crucial to highlight that the dual-Youla method could potentially introduce additional variance owing to this surplus order.

Chapter 4

The Two-Stage Identification

In the previous chapter, we have addressed the dual-Youla method, which guarantees the known controller always stabilizes the estimated plant. However, the dual-Youla estimate consists of two coprime factors that generally have higher orders than necessary, which may lead to additional errors due to overfitting. Therefore, we will consider another well-known indirect identification method, namely the Two-Stage method[10]. This method decomposes the closed-loop identification problem into two steps, each involving an open-loop problem. Opposed to the dual-Youla method, the two-stage method does not require the controller's knowledge, as the controller's information will be partially captured in the first stage and utilized to estimate the plant in the second stage. Similar to the last chapter, this chapter consists of three sections discussing the original method, the methodologies of our extended approach and eventually the implementation.

4.1 Fundamentals of Two-Stage Method

The two-stage method considers a system framework identical to the setup of the dual-Youla setup in Eq.3.1. This method starts by estimating the sensitivity function before identifying the plant. These two stages are explained in detail as follows.

- **Stage 1: Identification of the sensitivity function $\mathbf{T}_0$**

  The sensitivity function $\mathbf{T}_0$ is defined as the transfer function from $r(k)$ to $u(k)$, i.e.,

  $$u(k) = \mathbf{T}_0 r(k) + \mathbf{S}_0 e(k) \tag{4.1}$$

  Assuming the closed-loop system is asymptotically stable, i.e. the true sensitivity function $\mathbf{T}_0 \in \mathcal{RH}_\infty$, the estimate $\hat{\mathbf{T}}_N$ can be computed by solving the following problem,

  $$\hat{\mathbf{T}}_N = \underset{\mathbf{T}\in\mathcal{RH}_\infty}{\operatorname{argmin}} \ \|u(k) - \mathbf{T} r(k)\| \tag{4.2}$$

  Obviously, as $r(k)$ and $e(k)$ are independent, $\hat{\mathbf{T}}_N$ is a consistent estimate obtained by solving an equivalent open-loop identification problem, if certain conditions are satisfied[10]. Note the model order of $\mathbf{T}$ can be chosen arbitrarily since the plant model order will be independently determined in the next stage. In [10], the author suggests parameterizing $\mathbf{T}$ using an FIR representation. Note $\mathbf{T}_0$ is a rational transfer matrix; hence, FIR is merely an approximation and leads to truncation error. However, the bias is quantifiable and can be mitigated with a sufficiently large FIR order, as suggested by the author. Once the bias is considered small enough and thus negligible compared to the magnitude of the true parameters, we can claim the estimate is consistent and satisfactory.

- **Stage 2: Identification of the plant $\mathbf{G}_0$**

  In the second stage, we first approximate the noise-free input $u^r(k)$ by filtering the measured input $u(k)$ with the estimated sensitivity $\hat{\mathbf{T}}_N$ from the first stage,

  $$u^r(k) = \hat{\mathbf{T}}_N r(k) \tag{4.3}$$

  Then obtain the estimated plant $\hat{\mathbf{G}}_N$ as the transfer function from $u^r(k)$ to $y(k)$, which is equivalent to solving another open-loop problem,

  $$y(k) = \mathbf{G}_0 u^r(k) + (\mathbf{H}_0 + \mathbf{G}_0\mathbf{S}_0)e(k) \tag{4.4}$$

  $$\hat{\mathbf{G}}_N = \underset{\mathbf{G}\in\mathcal{R}_c}{\operatorname{argmin}} \ \|y(k) - \mathbf{G}u^r(k)\| \tag{4.5}$$

  With $u^r(k)$ only dependent on $r(k)$ thus uncorrelated with $e(k)$ by construction. $\hat{\mathbf{G}}_N$ is proved to be consistent, if the input is persistently exciting, the estimate $\hat{\mathbf{T}}_N$ is consistent, and the model structure of $\mathbf{G}$ is defined appropriately. Typically, one can choose from the framework of prediction error methods (such as least squares), or instrumental variables in case the noise dynamics are challenging to model.

4.2 Methodologies

Again, we aim at estimating $\mathbf{G}_0 \in \text{Sparse}(S)$ and pre-compute R via Algorithm 1. We further assume,

1). The excitation $r(k)$ is persistently exciting and statistically independent of the noise $e(k)$.

2). $\mathbf{G}_0$ is stabilizable and detectable, and the closed-loop has asymptotically stable dynamics.

3). $\mathbf{G}_0$ can be factorized into a pair of FIR filters that satisfy the sparsity constraints, i.e. $\exists \mathbf{A}_0, \mathbf{B}_0 \in \mathcal{F}_\tau$ s.t. $\mathbf{A}_0 \in \text{Sparse}(R),\ \mathbf{B}_0 \in \text{Sparse}(S),$ and $\mathbf{G}_0 = \mathbf{A}_0^{-1}\mathbf{B}_0$.

These essential assumptions ensure an invertible Hessian matrix in optimization, and the true model $\mathbf{G}_0$ is an element of the candidate set. With Assumption 1)., we can come up with the estimate of the sensitivity function $\hat{\mathbf{T}}_N$. Suppose an FIR parameterization with order ν is defined for $\mathbf{T}$, then Problem 4.2 becomes,

$$\hat{\mathbf{T}}_N = \underset{\mathbf{T}\in\mathcal{F}_\nu}{\operatorname{argmin}} \ \|u(k) - \mathbf{T}r(k)\| \tag{4.6}$$

This problem can be solved directly using prediction error methods, such as least squares. Hence, filtering $r(k)$ with $\hat{\mathbf{T}}_N$ based on Eq.4.3 gives an undisturbed input signal $u^r(k)$ that resembles the noise-free part of $u(k)$. Note in this stage, the sparsity constraints are not involved during the optimization in Eq.4.6, as we assume no knowledge about the controller or its structure either. Other reasons are the filtered signal $u^r(k)$ is already a decent approximation as long as $\mathbf{T}_N$ is consistent, while $\mathbf{T}_0$ is generally denser than $\mathbf{G}_0$ especially when the network is strongly connected. However, suppose the sparsity structure of $\mathbf{K}_0$ or even $\mathbf{T}_0$ is exactly known. In that case, we can use this information to restrict the number of variables, hence improving the estimation efficiency. In the case that $\mathbf{K}_0$ has a known structure, the sparsity constraints on $\mathbf{T}_0$ can be defined by,

$$\begin{aligned} &\mathbf{T}_0 = (I_{n_u} - \mathbf{K}_0\mathbf{G}_0)^{-1} \\ \Rightarrow\ &\mathbf{T}_0 \in \text{Sparse}\left((I_{n_u} + \text{Struct}(\mathbf{K}_0)\cdot\text{Struct}(\mathbf{G}_0))^{-1}\right) = \text{Sparse}(S_T) \end{aligned} \tag{4.7}$$

Problem 4.6 is further modified into,

$$\begin{aligned}\hat{\mathbf{T}}_N = \underset{\mathbf{T}\in\mathcal{F}_\nu}{\operatorname{argmin}} \ & \|u(k) - \mathbf{T}r(k)\| \\ \text{s.t. } & \mathbf{T} \in \text{Sparse}(S_T)\end{aligned} \tag{4.8}$$

After obtaining $\hat{\mathbf{S}}_N$ and computing $u^r(k)$, the next step is to construct the estimate $\hat{\mathbf{G}}_N$ using $y(k)$ and $u^r(k)$. We consider using a fractional representation to parameterize $\mathbf{G}$ so that the Sparsity Invariance Theorem is applicable. In other words, we suppose $\mathbf{G}_0 = \mathbf{A}_0^{-1}\mathbf{B}_0$ which leads to the open-loop dynamics as shown below,

$$\mathbf{A}_0 y(k) = \mathbf{B}_0 u^r(k) + \mathbf{L}_0 e(k), \quad \mathbf{L}_0 = \mathbf{A}_0\mathbf{H}_0 + \mathbf{B}_0\mathbf{S}_0 \tag{4.9}$$

Therefore, the sparsity-constrained two-stage identification yields the following optimization problem,

$$\begin{aligned}\hat{\mathbf{A}}_N, \hat{\mathbf{B}}_N = \underset{\mathbf{A},\mathbf{B}\in\mathcal{RH}_\infty}{\operatorname{argmin}} \ & \|\mathbf{A}y(k) - \mathbf{B}u^r(k)\| \\ \text{s.t. } & \mathbf{A} \in \text{Sparse}(R) \\ & \mathbf{B} \in \text{Sparse}(S) \\ & \mathbf{A} \text{ is invertible}\end{aligned} \tag{4.10}$$

And eventually $\hat{\mathbf{G}}_N = \hat{\mathbf{A}}_N^{-1}\hat{\mathbf{B}}_N$. Different from the sparsity filter $\mathbf{A}_Q$ defined in the extended dual-Youla method, the factor $\mathbf{A}$ is required to be invertible but not necessarily stably invertible. When $\mathbf{G}_0$ is known to be stable, a stable invertibility constraint could be an option to avoid introducing unstable poles. on the contrary, when there is no knowledge about the stability of $\mathbf{G}_0$, $\mathbf{A}_0^{-1}$ is probably unstable; thus, a stable invertibility constraint will lead to bias.
We define the invertibility of a transfer matrix $\mathbf{A}$ as that $\mathbf{A}$ has a causal inverse. For a square FIR transfer matrix, the causality of the inverse is implied by an invertible zeroth tap[23], i.e., A^0 is invertible where

$$\mathbf{A}(z) = A^0 + A^1 \cdot z^{-1} + \cdots + A^{\tau-1} \cdot z^{-(\tau-1)} \tag{4.11}$$

Therefore, the invertibility of $\mathbf{A}$ can be ensured by applying the Gershgorin Circle Theorem on A^0 in a fashion similar to Section 3.2.

4.3 Implementation

As mentioned previously, we will parameterize $\mathbf{T}$ with FIR representation with a sufficiently large order ν. In the example provided in [10], the author chooses ν about three times larger than the order of the true sensitivity function $\mathbf{T}_0$. Suppose $\mathbf{T}(\rho)$ is parameterized by a vector of variables ρ, which correspondingly yields the following structure,

$$\begin{aligned}&\mathbf{T}(\rho, z) = T^0 + T^1 \cdot z^{-1} + \cdots + T^\nu \cdot z^{-(\nu-1)} \\ \Rightarrow\ &\rho = \mathbf{vec}\left(\begin{bmatrix} T^0 & T^1 & \cdots & T^{\nu-1} \end{bmatrix}^\top\right)\end{aligned} \tag{4.12}$$

Hence, the dynamics from $r(k)$ to $u(k)$ can be written as,

$$
\begin{aligned}
u(k) &= \begin{bmatrix} T^0 & T^1 & \cdots & T^{\nu-1} \end{bmatrix} \cdot \begin{bmatrix} r(k) \\ r(k-1) \\ \vdots \\ r(k-\nu+1) \end{bmatrix} + \text{noise contribution} \\
\Rightarrow\ u(k) &= \Psi(k)^\top \rho \quad \text{where} \quad \Psi(k) = I_{n_u} \bigotimes \begin{bmatrix} r(k) \\ r(k-1) \\ \vdots \\ r(k-\nu+1) \end{bmatrix}
\end{aligned} \tag{4.13}
$$

Therefore, staking $\Psi(k)$ and $u(k)$ leads to an LS estimate $\hat{\rho}_N^{LS}$,

$$
\boldsymbol{\Psi} = \begin{bmatrix} \Psi(0)^\top \\ \Psi(1)^\top \\ \vdots \\ \Psi(N-1)^\top \end{bmatrix} \quad \mathbf{u} = \begin{bmatrix} u(0) \\ u(1) \\ \vdots \\ u(N-1) \end{bmatrix} \ \Rightarrow\ \hat{\rho}_N^{LS} = \left(\boldsymbol{\Psi}^\top \boldsymbol{\Psi}\right) \boldsymbol{\Psi}^\top \mathbf{u} \tag{4.14}
$$

We are now able to construct $\hat{\mathbf{T}}_N^{LS}$ and $u^r(k)$ according to Eq.4.12 and Eq.4.3 respectively. Moving on, we choose the ARX model with order τ for both the denominator and numerator as the fractional representation for $\mathbf{G} = \mathbf{A}^{-1}\mathbf{B}$, by defining the factors as follows,

$$
\begin{aligned}
\mathbf{A}(z) &= I_{n_y} + A^1 \cdot z^{-1} + \cdots A^\tau \cdot z^{-(\tau-1)} = I_{n_y} + z^{-1} \cdot \mathbf{A}^*(z) \\
\mathbf{B}(z) &= B^0 + B^1 \cdot z^{-1} + \cdots B^\tau \cdot z^{-(\tau-1)}
\end{aligned} \tag{4.15}
$$

Correspondingly, by independently parameterizing $\mathbf{A}$, $\mathbf{B}$ with θ and $\mathbf{L}$ with η, the open-loop dynamics is rewritten into,

$$
\begin{aligned}
&\mathbf{A}(\theta) y(k) = \mathbf{B}(\theta) u^r(k) + \mathbf{L}(\eta) e(k) \\
\Rightarrow\ &y(k) = -\mathbf{A}^*(\theta) y(k-1) + \mathbf{B}(\theta) u^r(k) + \mathbf{L}(\eta) e(k)
\end{aligned} \tag{4.16}
$$

Which results in another LS problem,

$$
\hat{\theta}_N^{LS} = \underset{\theta}{\operatorname{argmin}}\ \|\mathbf{y} - \boldsymbol{\Phi}\theta\| = \left(\boldsymbol{\Phi}^\top \boldsymbol{\Phi}\right)^{-1} \boldsymbol{\Phi}^\top \boldsymbol{y} \tag{4.17}
$$

With the regressor matrices and label vectors defined as,

$$
\Phi(k) = \begin{bmatrix} -I_{n_y} \bigotimes \begin{bmatrix} y(k-1) \\ y(k-2) \\ \vdots \\ y(k-\tau+1) \end{bmatrix} \\ I_{n_y} \bigotimes \begin{bmatrix} u^r(k) \\ u^r(k-1) \\ \vdots \\ u^r(k-\tau+1) \end{bmatrix} \end{bmatrix}, \quad \boldsymbol{\Phi} = \begin{bmatrix} \Phi(0)^\top \\ \Phi(1)^\top \\ \vdots \\ \Phi(N-1)^\top \end{bmatrix}, \quad \boldsymbol{y} = \begin{bmatrix} y(0) \\ y(1) \\ \vdots \\ y(N-1) \end{bmatrix} \tag{4.18}
$$

The sparsity constraints $\mathbf{A} \in \text{Sparse}(R)$ and $\mathbf{B} \in \text{Sparse}(S)$ are implemented similar to those in the dual-Youla setup, but in a much simpler manner:

$$
\begin{aligned}
&\tilde{\mathbf{E}}_R = I_{(\tau-1)\cdot n_y^2} \quad \mathbf{R} = \begin{bmatrix} R & R & \cdots & R \end{bmatrix} \ \Rightarrow\ \mathbf{E}_R = \tilde{\mathbf{E}}_R \left(\mathbf{vec}\left(\mathbf{R}^\top\right) == 0\right) \\
&\tilde{\mathbf{E}}_S = I_{\tau \cdot n_y \cdot n_u} \quad \mathbf{S} = \begin{bmatrix} S & S & \cdots & S \end{bmatrix} \ \Rightarrow\ \mathbf{E}_S = \tilde{\mathbf{E}}_S \left(\mathbf{vec}\left(\mathbf{S}^\top\right) == 0\right) \\
\Rightarrow\ &\mathbf{E} = \begin{bmatrix} \mathbf{E}_R \\ \mathbf{E}_S \end{bmatrix}
\end{aligned} \tag{4.19}
$$

The sparsity-constrained least squares problem is then formulated as,

$$\begin{aligned} &\min_{\theta} \ \|\mathbf{y} - \mathbf{\Phi}\theta\| \\ &\text{s.t. } \mathbf{E}\theta = \mathbf{0} \end{aligned} \tag{4.20}$$

Leading to the constrained least squares solution with $\mathbf{P} = \mathbf{\Phi}^\top \mathbf{\Phi}$ identical to Eq.3.34,

$$\begin{aligned} \hat{\theta}_N^{CLS} &= \left[\mathbf{P}^{-1} - \mathbf{P}^{-1}\mathbf{E}^\top \left(\mathbf{E}\mathbf{P}^{-1}\mathbf{E}^\top\right)^\dagger \mathbf{E}\mathbf{P}^{-1}\right] \mathbf{\Phi}^\top \boldsymbol{y} \\ &= \hat{\theta}_N^{LS} - \mathbf{P}^{-1}\mathbf{E}^\top \left(\mathbf{E}\mathbf{P}^{-1}\mathbf{E}^\top\right)^\dagger \mathbf{E} \cdot \hat{\theta}_N^{LS} \end{aligned} \tag{4.21}$$

Which minimizes the model fitting error and guarantees that $\hat{\mathbf{G}}_N^{CLS}$ satisfies the sparsity constraints. Similarly, the regularized constraint least squares solution considering a ℓ_2 norm regularization with a penalizing constant λ is given by,

$$\begin{aligned} &\hat{\theta}_N^{RCLS} = \left[\mathbf{P}(\lambda)^{-1} - \mathbf{P}(\lambda)^{-1}\mathbf{E}^\top \left(\mathbf{E}\mathbf{P}(\lambda)^{-1}\mathbf{E}^\top\right)^\dagger \mathbf{E}\mathbf{P}(\lambda)^{-1}\right] \mathbf{\Phi}^\top \boldsymbol{y} \\ &\text{where} \quad \mathbf{P}(\lambda) = \mathbf{\Phi}^\top\mathbf{\Phi} + \mathbf{\Lambda}(\lambda), \ \ \mathbf{\Lambda}(\lambda) = \begin{bmatrix} \lambda \cdot I_{(\tau-1)\cdot n_y^2} & \mathbf{0} \\ \mathbf{0} & \mathbf{0} \end{bmatrix} \end{aligned} \tag{4.22}$$

As explained previously, the RCLS estimate $\hat{\theta}_N^{RCLS}$ is preferred when $\mathbf{G}_0$ is known to be stable but $\hat{\theta}_N^{CLS}$ unfortunately results in an unstable inverse of $\hat{\mathbf{A}}_N^{CLS}$. It is worth noting that the framework of least squares estimates on the two-stage method can provide an unbiased and consistent estimate only if the following is true with i.i.d. noise $e(k)$,

$$\mathbf{A}_0 y(k) = \mathbf{B}_0 u^r(k) + e(k) \ \text{ i.e. } \mathbf{L}_0 = I_{n_y} \text{ in Eq.4.9} \tag{4.23}$$

Which is almost impossible. Therefore, when a consistent estimate is required, we have to seek help from other methods rather than merely using least squares. A possible alternative is again the instrumental variables. The instruments $\zeta(k)$ can be generated by filtering the undisturbed input $u^r(k)$ with the LS estimate of the plant,

$$\hat{\theta}_N^{LS} \text{ by Eq.4.17} \ \ \Rightarrow \ \ \hat{\mathbf{G}}_N^{LS} \ \ \Rightarrow \ \ \zeta(k) = \hat{\mathbf{G}}_N^{LS} u^r(k) \tag{4.24}$$

Before constructing the instrument matrix,

$$Z(k) = \begin{bmatrix} -I_{n_y} \bigotimes \begin{bmatrix} \zeta(k-1) \\ \zeta(k-2) \\ \vdots \\ \zeta(k-\tau+1) \end{bmatrix} \\ I_{n_y} \bigotimes \begin{bmatrix} u^r(k) \\ u^r(k-1) \\ \vdots \\ u^r(k-\tau+1) \end{bmatrix} \end{bmatrix} \ \Rightarrow \ \mathbf{Z} = \begin{bmatrix} Z(0)^\top \\ Z(1)^\top \\ \vdots \\ Z(N-1)^\top \end{bmatrix} \tag{4.25}$$

Finally, reusing the definition of $\mathbf{\Phi}$, $\mathbf{y}$ in Eq.4.18 and $\mathbf{E}$ in Eq.4.19, the constrained instrumental variables solution is expressed as,

$$\hat{\theta}_N^{CIV} = \left[\left(\mathbf{Z}^\top\mathbf{\Phi}\right)^{-1} - \left(\mathbf{Z}^\top\mathbf{\Phi}\right)^{-1}\mathbf{E}^\top \left(\mathbf{E}\left(\mathbf{Z}^\top\mathbf{\Phi}\right)^{-1}\mathbf{E}^\top\right)^\dagger \mathbf{E}\left(\mathbf{Z}^\top\mathbf{\Phi}\right)^{-1}\right] \mathbf{Z}^\top \boldsymbol{y} \tag{4.26}$$

Which is now theoretically unbiased and consistent, while the resultant $\hat{\mathbf{G}}_B^{CIV}$ satisfies the sparsity constraints as well. The proof is identical to Section 3.3.4, thus omitted here.

Chapter 5

Results and Discussion

This chapter aims to illustrate the identification framework's application in real-world problem-solving as a means of verification. To achieve this, we have selected two networked systems to represent distinct scenarios. We have simulated their behaviors using predefined excitation signals, collected noisy data from closed-loop operations, and subsequently employed this data to identify the underlying plant.

Specifically, the chosen system is a moderately scaled unstable irrigation network, as previously studied in the work of [24]. In their research, the authors introduce a linear model to approximate the system dynamics and successfully figure out a functional controller for practical application. Given that modeling irrigation networks is inherently complicated, as acknowledged by the authors, pursuing an identification method that can provide an effective system approximation is of great importance. Note this irrigation network is intrinsically unstable; hence only the extended dual-Youla method is applied, attributed to its stabilizability guarantee on the identified plant.

To fully demonstrate our simulation results, this chapter consists of two sections. Section 5.1 provides a comprehensive overview of the example system and outlines the data generation to facilitate the identification process. In Section 5.2, we apply the proposed method to the example system and present the variation in estimates across different scenarios, which helps assess the performance of the extended framework.

5.1 System Specification

Prior to data generation, it is essential to comprehend the system dynamics. Similar to the setup in [24], we assume that the irrigation network consists of n individual pools in series. Each pool i possesses its water level denoted as $y_i(t)$, subject to interference from an unobservable yet identically and independently distributed (i.i.d.) disturbance $d_i(t)$. The management of the water level is governed by the flow over the pool gate, defined as the input $u_i(t)$, serving the subsequent purpose:

- Reject disturbances and stabilizes $y_i(t)$;
- Regulate $y_i(t)$ to a given reference set-point $r_i(t)$ with zero steady-state error, i.e. the level error $e_i(t) = r_i(t) - y_i(t)$ converges to 0 as $t \to \infty$.

Apparently, employing a conventional Proportional plus Integral (PI) compensator can lead to stabilization and zero-error regulation. As suggested in the original paper[24], the most straightforward configuration is the decentralized control, wherein each individual plant is equipped with

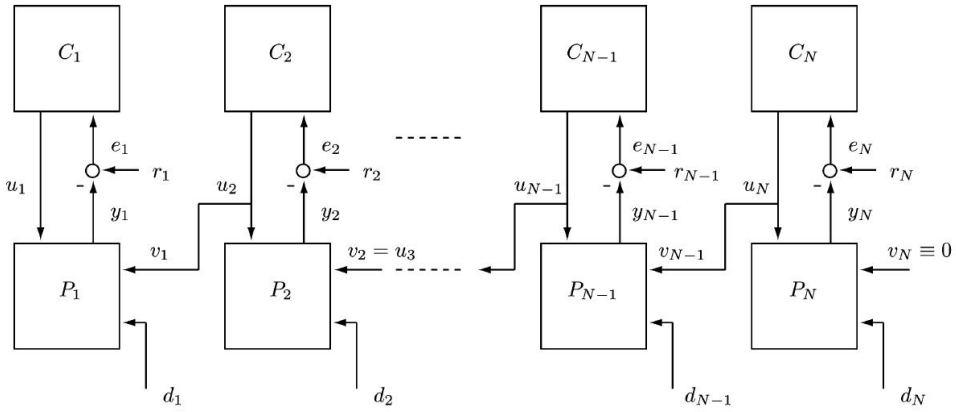

Figure 5.1: Schematic representation of the irrigation system under decentralized control[24].

its local compensator denoted as $C_i(s)$. The architecture of the decentralized control system is given in Fig.5.1. The dynamics of the system can be expressed as,

$$\begin{aligned} y_i(t) &= \frac{\exp(-\kappa_i s)}{\alpha_i s} \cdot u_i(t) - \frac{1}{\alpha_i s} \cdot u_{i+1}(t) + d_i(t) \\ u_i(t) &= C_i(s) e_i(t) = \frac{\gamma_i(1+\phi_i s)}{s(1+\rho_i s)} \cdot (r_i(t) - y_i(t)) \end{aligned} \tag{5.1}$$

With κ_i the input delay and α_i the pool surface area. Other constants γ_i, ϕ_i and ρ_i are controller parameters to be tuned for each compensator. As the author suggests employing a Pade approximation to replace the time-delay term $\exp(-\kappa_i s)$, we consider the following expression to describe the IO channel $P_{ii}(s)$ for each pool,

$$\frac{\exp(-\kappa_i s)}{\alpha_i s} \approx \frac{-\kappa_i s + 2}{\alpha_i s(\kappa_i s + 2)} = P_{ii}(s) \tag{5.2}$$

This is valid since the system exhibits slow dynamics (pools have substantial surface areas) thus low frequencies are of more interest. The choice of the parameters will be discussed in Section 5.1.1.

5.1.1 Plant and Controller

We first denote the entire interconnected plant as $\mathbf{P}(s) \in \mathcal{R}_c^{n\times n}$, the output vector $y(t) = [y_1(t), y_2(t), \cdots, y_n(t)]^\top \in \mathbb{R}^n$ and same for $u(t), r(t), e(t), d(t) \in \mathbb{R}^n$, then $y(t) = \mathbf{P}(s)u(t) + d(t)$. Consequently,

$$\begin{aligned} \mathbf{P}(s) &= \begin{bmatrix} P_{11}(s) & P_{12}(s) & 0 & \cdots & 0 \\ 0 & P_{22}(s) & P_{23}(s) & \cdots & 0 \\ \vdots & \vdots & \ddots & \ddots & \vdots \\ 0 & 0 & 0 & \cdots & P_{(n-1)n}(s) \\ 0 & 0 & 0 & \cdots & P_{nn}(s) \end{bmatrix} \\ &= \begin{bmatrix} \frac{\exp(-\kappa_1 s)}{\alpha_1 s} & -\frac{1}{\alpha_1 s} & 0 & \cdots & 0 \\ 0 & \frac{\exp(-\kappa_2 s)}{\alpha_2 s} & -\frac{1}{\alpha_2 s} & \cdots & 0 \\ \vdots & \vdots & \ddots & \ddots & \vdots \\ 0 & 0 & 0 & \cdots & -\frac{1}{\alpha_{n-1} s} \\ 0 & 0 & 0 & \cdots & \frac{\exp(-\kappa_n s)}{\alpha_n s} \end{bmatrix} \end{aligned} \tag{5.3}$$

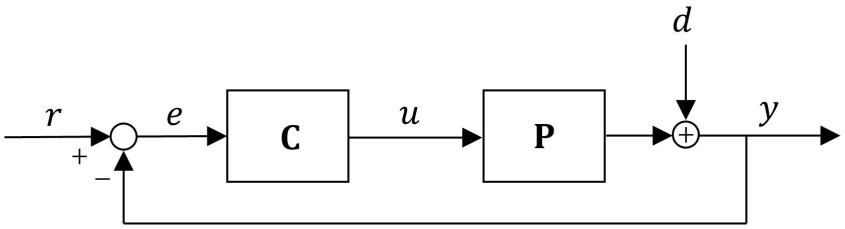

Figure 5.2: Compact block diagram of the MIMO irrigation system.

Eq.5.3 indicates the plant sparsity structure $S_n = \text{Struct}\,(\mathbf{P}(s))$ is an upper bidiagonal binary matrix with dimension n. For instance, if the irrigation network has $n = 5$ nodes, then

$$S_5 = \begin{bmatrix} 1 & 1 & 0 & 0 & 0 \\ 0 & 1 & 1 & 0 & 0 \\ 0 & 0 & 1 & 1 & 0 \\ 0 & 0 & 0 & 1 & 1 \\ 0 & 0 & 0 & 0 & 1 \end{bmatrix} \quad \Rightarrow \quad R_5 = \begin{bmatrix} 1 & 0 & 0 & 0 & 0 \\ 0 & 1 & 0 & 0 & 0 \\ 0 & 0 & 1 & 0 & 0 \\ 0 & 0 & 0 & 1 & 1 \\ 0 & 0 & 0 & 0 & 1 \end{bmatrix} \text{ by Algorithm 1.} \tag{5.4}$$

The block diagram is displayed in Fig.5.2. Besides, we denote the MIMO controller as $\mathbf{C}(s)$ s.t. $u(t) = \mathbf{C}(s)e(t)$. Hence,

$$\mathbf{C}(s) = \begin{bmatrix} C_1(s) & 0 & \cdots & 0 \\ 0 & C_2(s) & \cdots & 0 \\ \vdots & \vdots & \ddots & \vdots \\ 0 & 0 & \cdots & C_n(s) \end{bmatrix} \tag{5.5}$$

For simplicity, we consider all the pools identical, and we use the same compensators for each pool to streamline the controller structure. Hence, $P_{ii}(s) = P(s)$, $C_{ii}(s) = C(s)$ and $P_{i(i+1)}(s) = Q(s)$ for all pools. This assumption does not compromise generality, as the scope of this report does not encompass controller design, nor do we employ the knowledge of identical pools; hence, the identification method works as if all individual plants are different. Moreover, we discretize the plant using the first-order forward Euler given a sampling time T_s,

$$\frac{1}{s} \;\rightarrow\; \frac{T_s}{z-1} \tag{5.6}$$

Therefore, the channels obey the following discretization rules,

$$\begin{aligned} P(s) &= \frac{-\kappa s + 2}{\alpha s(\kappa s + 2)} \;\rightarrow\; P(z) = \frac{-\frac{\kappa}{T_s}(z-1) + 2}{\frac{\alpha}{T_s}(z-1)\left(\frac{\kappa}{T_s}(z-1) + 2\right)} \\ Q(s) &= \frac{1}{\alpha s} \;\rightarrow\; Q(z) = \frac{1}{\frac{\alpha}{T_s}(z-1)} \end{aligned} \tag{5.7}$$

Motivated by the real examples examined in [24], we opt for values of $\alpha = 1$ [ha] $= 10^4$ [m^2], $\kappa = 2$ [min], and the sampling time is chosen as $T_s = 1$ [min]. We consider $n = 5$ pools to construct a moderately scaled plant. Consequently, the transfer functions $P(z)$, $Q(z)$ and the stabilizing compensator $C(s)$ are given by,

$$P(z) = -\frac{z-2}{z(z-1)} \quad Q(z) = -\frac{1}{z-1} \quad C(z) = \frac{0.15(z-0.95)}{(z-1)(z-0.1)} \tag{5.8}$$

Since both $P(z)$ and $Q(z)$ contain an integrator, the entire plant $\mathbf{P}(z)$[1] have unstable IO dynamics. As a remedy, the chosen MIMO controller $\mathbf{C}(z)$ managed to asymptotically stabilize the

[1]In the subsequent sections of this chapter, we no longer consider the continuous-time configuration. All bold symbols with or without (z) represent discrete-time transfer matrices.

plant while enforcing the output to perform error-free steady-state tracking. Hence, we define the entire plant and controller in discrete-time as,

$$\begin{aligned}
\mathbf{P}(z) &= \begin{bmatrix} P(z) & Q(z) & 0 & 0 & 0 \\ 0 & P(z) & Q(z) & 0 & 0 \\ 0 & 0 & P(z) & Q(z) & 0 \\ 0 & 0 & 0 & P(z) & Q(z) \\ 0 & 0 & 0 & 0 & P(z) \end{bmatrix} \\
\mathbf{C}(z) &= \begin{bmatrix} C(z) & 0 & 0 & 0 & 0 \\ 0 & C(z) & 0 & 0 & 0 \\ 0 & 0 & C(z) & 0 & 0 \\ 0 & 0 & 0 & C(z) & 0 \\ 0 & 0 & 0 & 0 & C(z) \end{bmatrix}
\end{aligned} \tag{5.9}$$

Followed by the MIMO dynamics,

$$\begin{aligned}
y(k) &= \mathbf{P}(z)u(k) + d(k) \\
u(k) &= \mathbf{C}(z)e(k) = \mathbf{C}(z) \cdot (r(k) - y(k))
\end{aligned} \tag{5.10}$$

And we denote the true plant, the known controller, and the estimated plant is given data length N as $\mathbf{P}_0$, $\mathbf{C}_0$ and $\hat{\mathbf{P}}_N$, respectively.

5.1.2 Signal Processing

Within this section, our objective is to establish the excitation reference $r(k)$ and the external disturbance $d(k)$, while defining several concepts that will be used to quantify the estimation outcomes.

- **Excitation reference**

  For identification purposes, the PRBS signal [25] emerges as a common preference for exciting the system, due to its deterministic nature combined with statistical characteristics similar to the truly random binary sequence. Therefore, we choose the PRBS signal as the excitation to generate the data for identification purposes and name it the training reference. We will assess the consistency of the identification method over a wide range of excitation lengths N, and the quality of the estimation is expected to improve with larger values of N. We define $r^0(k) = \text{PRBS}(N, n)$ as the nominal excitation signal with a magnitude of 1, equivalent to 0 in [dB]. Statistically, $\mathbb{E}[r^0(k)] = \mathbf{0}$ and $\mathbf{Var}(r^0(k)) = I_n$, which means the reference signals for distinct pools are independent.

  Furthermore, a magnified excitation reference, such as $r^{10}(k)$, represents a PRBS signal with a 10 [dB] amplification, achieved by multiplying the nominal excitation $r^0(k)$ by a constant. These magnified excitation signals will be utilized to evaluate the identification performance across various signal-to-noise ratios. We further choose the RBS signal or white noise as the validation reference, which is denoted as $r^{val}(k)$ and used to construct the validation output $y^{val}(k)$ by,

  $$y^{val}(k) = (I_n - \mathbf{P}_0\mathbf{C}_0)^{-1}\,\mathbf{P}_0\mathbf{C}_0 \cdot r^{val}(k) \tag{5.11}$$

  Later on, we will use $r^{val}(k)$ and $y^{val}(k)$ as validation data to examine $\hat{\mathbf{P}}_N$.

- **Signal-to-noise ratio**

  The signal-to-noise ratio (SNR) commonly serves as a standard depiction of the power relationship between useful signals and the effect of noise. It is distinctly defined for every

output $y_i(k)$ as the ratio of signal power to noise power. In a more detailed context, we first decompose the output into two components in accordance with the linearity of the system,

$$y(k) = \mathbf{W}(z)r(k) + \mathbf{X}(z)d(k) = y^r(k) + y^d(k) \tag{5.12}$$

With $\mathbf{x}(z)$ the closed-loop transfer matrix from $r(k)$ to $y(k)$ and $\mathbf{X}(z)$ from $d(k)$ to $y(k)$. Hence, for each individual pool, the SNR is computed by,

$$\mathrm{SNR}_i = \frac{\mathbf{Var}\left(y_i^r(k)\right)}{\mathbf{Var}\left(y_i^d(k)\right)} \tag{5.13}$$

A larger SNR indicates more valuable information we can obtain from the signal and theoretically results in a better estimate.

- **External disturbance**

  Conventionally, the disturbance signal is chosen to obey the standard normal distribution with a mean of zero and a variance of one, denoted as $d^0(k) \sim \mathcal{N}(\mathbf{0}, I_n)$. Nevertheless, owing to the interconnections among channels within the system, achieving a consistent SNR across all outputs is generally impossible when employing identical disturbance levels. Consequently, we must ascertain the disturbance magnitude for each distinct output i to ensure they collectively exhibit a uniform SNR value. More specifically, we want to figure out a diagonal weight matrix $M \in \mathbb{R}^{n\times n}$ and let $d(k) = M \cdot d^0(k)$, so that $\mathrm{SNR}_1 \approx \mathrm{SNR}_2 \approx \cdots \approx \mathrm{SNR}_n \approx 1$ when $r^0(k)$ is used to excite the system while $d(k)$ is the disturbance. The weight matrix is computed as follows. We first expand Eq.5.12,

$$y(k) = \mathbf{W}(z)r(k) + \mathbf{X}(z)d(k) = \mathbf{W}(z)r(k) + \mathbf{X}(z) \cdot M \cdot d^0(k) \tag{5.14}$$

  Thus for each node i, suppose the standard $r^0(k)$ is used as the reference signal,

$$\begin{aligned} y_i(k) = y_i^r(k) + y_i^d(k) &= \sum_j^n W_{ij}(z) r_j^0(k) + \sum_j^n X_{ij}(z) M_j d_j^0(k) \\ &= \sum_j^n y_{ij}^{r0}(k) + \sum_j^n M_j \cdot y_{ij}^{d0}(k) \end{aligned} \tag{5.15}$$

  Where M_j stands for the j-th diagonal of M and $y_{ij}^{r0}(k)$ represents the contribution of $r_j^0(k)$ to $y_i(k)$. The equation in Eq.5.15 can be rewritten into the following system of equations,

$$\begin{bmatrix} \mathbf{Var}\left(y_{11}^{d0}(k)\right) & \cdots & \mathbf{Var}\left(y_{1n}^{d0}(k)\right) \\ \vdots & \ddots & \vdots \\ \mathbf{Var}\left(y_{n1}^{d0}(k)\right) & \cdots & \mathbf{Var}\left(y_{nn}^{d0}(k)\right) \end{bmatrix} \begin{bmatrix} M_1 \\ \vdots \\ M_n \end{bmatrix} = \begin{bmatrix} \sum_{j=1}^n \mathbf{Var}\left(y_{1j}^{r0}(k)\right) \\ \vdots \\ \sum_{j=1}^n \mathbf{Var}\left(y_{nj}^{r0}(k)\right) \end{bmatrix} \tag{5.16}$$

  The data sequences $y_{ij}^{r0}(k)$ and $y_{ij}^{d0}(k)$ can be generated through simulating the system using only $r_j^0(k)$ or $d_j^0(k)$, respectively. Typically, the matrix on the left-hand side of Eq.5.16 is invertible due to the stronger correlation between $y_i(k)$ and $d_i(k)$ compared to that between $y_i(k)$ and $d_j(k)$ for $i \neq j$. We now possess the capability to manipulate the SNR by adjusting the reference level, while ensuring that all outputs maintain similar SNR values using the weight above matrix M to obtain the scaled disturbance $d(k)$.

- **Root mean squared error**

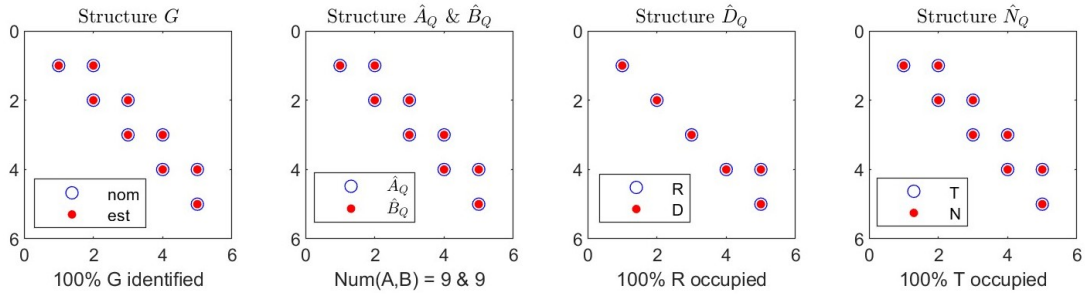

Figure 5.3: The five-node identification sparsity plot.

Finally, we introduce the root mean squared error (RMSE) as a quantitative tool to assess the accuracy of the estimated model. As discussed earlier, we can select a distinct validation reference $r^{val}(k)$, differing from $r^0(k)$, and simulate the system without disturbances to derive $y^{val}(k)$. Additionally, after acquiring an estimation $\hat{\mathbf{P}}_N$, we can formulate the predicted output by employing the following expression:

$$\hat{y}(k) = \left(I_n - \hat{\mathbf{P}}_N \mathbf{C}_0\right)^{-1} \hat{\mathbf{P}}_N \mathbf{C}_0 \cdot r^{val}(k) \tag{5.17}$$

Then, we define the RMSE for the estimate as,

$$\text{RMSE} = \sqrt{\frac{\frac{1}{N \cdot n} \sum_{k=0}^{N-1} \|\hat{y}(k) - y^{val}(k)\|_2^2}{\frac{1}{N \cdot n} \sum_{k=0}^{N-1} \|y^{val}(k)\|_2^2}} \times 100\% \tag{5.18}$$

As we progressively increase N or SNR to attain a new estimate $\hat{\mathbf{P}}_N$, we expect a gradual reduction in RMSE, which is indicative proof of a consistent and unbiased estimate.

5.2 Simulation

Within this section, we will present the results achieved through the identification of the plant using the dual-Youla parameterization, by assuming a trivial initial guess $\mathbf{G}_X = \mathbf{0}$, owing to its advantage of guarantee on the stabilizability of the estimated plant. Furthermore, we will conduct a comparative analysis of these results and engage in subsequent discussions.

In the example, the control system used for simulations has $n = 5$ nodes characterized by transfer functions specified in Equation 5.8, along with the architecture described in Equation 5.9. We stimulate the system with a PRBS signal being the excitation reference while concurrently corrupting the measured output with normally distributed disturbances, as elaborated in Section 5.1.2. As an example to provide a general figure regarding the identification performance, we first demonstrate the CLS[2] estimate with $N = 1023$, SNR $= 0$ [dB], model order $\tau = 8$. Fig.5.3 is defined as the sparsity plot which visualizes the sparsity patterns[3] of the nominal plant, the estimated plant and the factors used to construct the estimate.
Please note the notations of these transfer matrices:

$$\begin{aligned}
\mathbf{Q} &= \mathbf{A}_Q^{-1} \mathbf{B}_Q \\
\mathbf{D}_Q &= \mathbf{A}_Q \mathbf{D}_X + \mathbf{B}_Q \mathbf{N}_K \\
\mathbf{N}_Q &= \mathbf{A}_Q \mathbf{N}_X + \mathbf{B}_Q \mathbf{D}_K \\
\mathbf{G} &= \mathbf{D}_Q^{-1} \mathbf{N}_Q
\end{aligned} \tag{5.19}$$

[2]In this example, $\hat{\mathbf{A}}_Q^{CLS}$ is already stably invertible, hence the regularizer is unnecessary.
[3]Achieved by the command **spy**$(\cdot)$ in MATLAB.

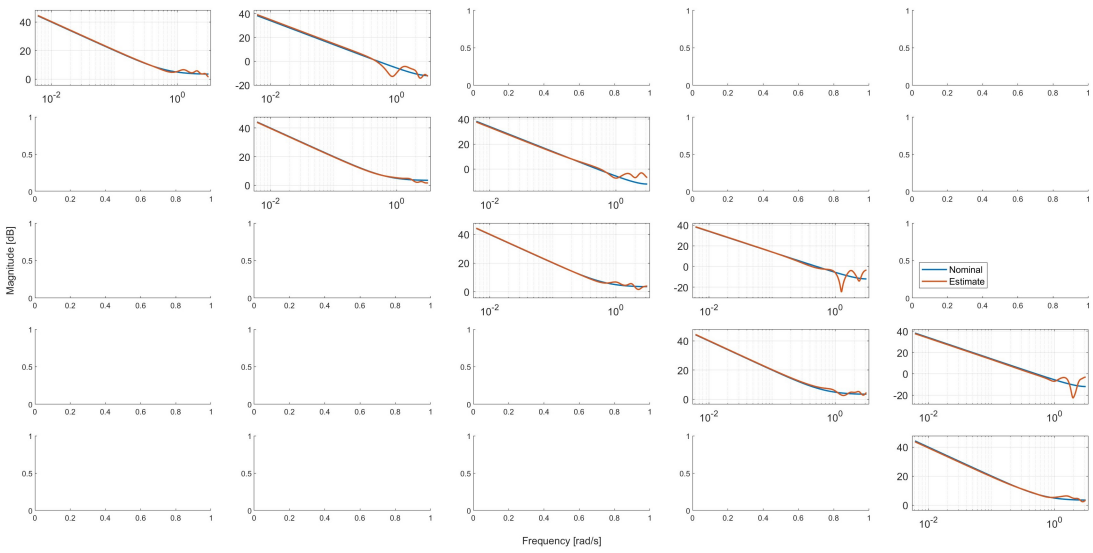

Figure 5.4: Magnitude response of the estimated plant with $N = 1023$, SNR $= 0$ [dB] and $\tau = 8$, compared with the true plant. An empty plot indicates no transfer functions defined (sparsity).

In particular, the first left subgraph of Figure 5.3 presents the nominal sparsity pattern S defined in Eq.5.4 and denoted by blue circles. At the same time, the estimated plant has a sparsity pattern depicted by red dots. Evidently, the estimated plant replicates the same sparsity pattern as the nominal one, implying that $\text{Struct}(\hat{\mathbf{G}}) = S$. Subsequently, the second graph on the left illustrates the compositions of the ARX factors of $\hat{\mathbf{Q}}$, which, even though not directly restricted by the sparsity constraints, still manifest specific sparsity characteristics.

Moving to the right side, the two remaining graphs depict the configurations of the denominator $\hat{\mathbf{D}}_Q$ and numerator $\hat{\mathbf{N}}_Q$ of $\hat{\mathbf{G}}$. Both transfer matrices conform to the intended sparsity subspaces such that $\mathbf{D}_Q \in \text{Sparse}(R)$ and $\mathbf{N}_Q \in \text{Sparse}(S)$. As these conditions are met, we can confidently assert that the algorithm triumphs in recovering the correct sparsity structure.
We continuously examine the properties of the estimation. The magnitude response plot of all channels is presented in Figure 5.4 with the response of the nominal plant $\mathbf{G}_0$ in blue and that of the estimate $\hat{\mathbf{G}}$ in red. As illustrated by the sparsity plot in Figure 5.3, the identified plant exhibits an upper bidiagonal sparsity pattern that aligns precisely with the nominal plant. This alignment is evident by the absence of any magnitude response in regions where the channel is zero within $\mathbf{G}_0$. Besides, it is obvious that, at lower frequencies, all channels exhibit decent alignments between the nominal and the estimated plants. However, there is a noticeable deviation at high frequencies, for which a plausible explanation is an excessively high model order selection, possibly inducing overfitting in the high frequencies. Despite this, the estimation generally demonstrates a propensity to converge towards the true magnitude response.
We will then keep exploring the variations in estimation performance by sequentially varying the SNR from 0 to 40 [dB], the data length N over the range of 511 to 131071, adjusting the model order from 3 to 16, and comparing the sparsity-constrained estimates with the free ones (i.e., without sparsity constraints). As the sparsity plots for all estimates remain identical when the sparsity constraints are active, they are omitted in the following subsections.

5.2.1 Varying Signal-to-Noise Ratio and Data Length

The following figure and table illustrate the variations in RMSE as a function of increasing N or SNR. In the table on the right, the leftmost column corresponds to different values of N, while

the topmost row corresponds to different SNR levels in decibels. The main section of the table contains the RMSE values represented in percentage.

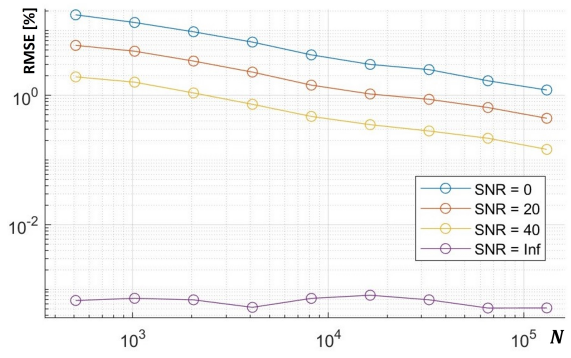

Figure 5.5: RMSE [%] vs. N and SNR.

N\SNR	0	20	40	Inf
511	17.6	5.93	1.93	6.7E-04
1023	13.4	4.82	1.6	7.3E-04
2047	9.62	3.39	1.09	6.9E-04
4095	6.67	2.29	0.727	5.3E-04
8191	4.23	1.44	0.462	7.2E-04
16383	3.01	1.05	0.352	8.1E-04
32767	2.5	0.868	0.281	6.9E-04
65535	1.68	0.648	0.217	5.1E-04
131071	1.21	0.442	0.146	5.2E-04

Table 5.1: RMSE [%] vs. N and SNR.

Obviously, when operating under a finite SNR, all the estimates demonstrate an asymptotic convergence of the root mean squared error (RMSE), with a decrease rate of $\mathcal{O}(N^{1/2})$. This trend is rational since, conventionally, the covariance matrix of the estimate scales inversely with the data length[2], as can be expressed as follows:

$$\mathbf{Var}\left(\hat{\mathbf{G}}\right) \sim \frac{\tau}{N}\frac{\Phi_d}{\Phi_u^r} \tag{5.20}$$

Here, Φ_d signifies the power spectrum of the disturbance, and Φ_u^r represents the power of control inputs emerging from reference signals. Furthermore, as the SNR increases, the entire curve shifts downwards, approaching the noise-free scenario where negligible numerical errors primarily influence the RMSE. To provide a more comprehensive visualization of the impact of increasing SNR and N, we present the Bode diagrams of the estimated channel $\hat{\mathbf{G}}_{11}$ alongside the nominal channel. These diagrams are showcased in Fig.5.6 for different SNR values and in Fig.5.7 for different N values. Both figures clearly demonstrate that in extreme cases, such as when dealing with high SNR or considerably large N values, the deviation between the estimated and nominal channels becomes nearly invisible. This indicates the consistency of the proposed method in generating output predictions, at least within the data length range from 10^2 to 10^5.

The outcomes remain notable despite the theoretical biases and inconsistencies associated with the least-squares method, as discussed in Section 3.3.4. Through a relatively straightforward algorithm that addresses a quadratic program, we achieve consistent output predictions and a commendable model approximation. This is particularly evident when evaluating the RMSE at $N = 32767$ and SNR $= 20$ dB, which already falls below 1%. Consequently, we are warranted in concluding that the proposed method is both satisfactory and effective, if the model order is chosen appropriately, as will be discussed in the following subsection.

5.2.2 Varying Model Order

The model order τ as a hyperparameter can significantly influence the performance of the estimator. Striking a balance is crucial since setting τ excessively high could burden computational complexity, while opting for an aggressively small τ might exclude the true model from the candidate set, thereby introducing bias. Typically, the choice of τ depends on the a-prior knowledge of the system architecture or can be tuned via cross-validation or other mature equivalent methods. To demonstrate the effect of choosing the model order, the following graph and table display the variation in RMSE w.r.t. both N and τ.

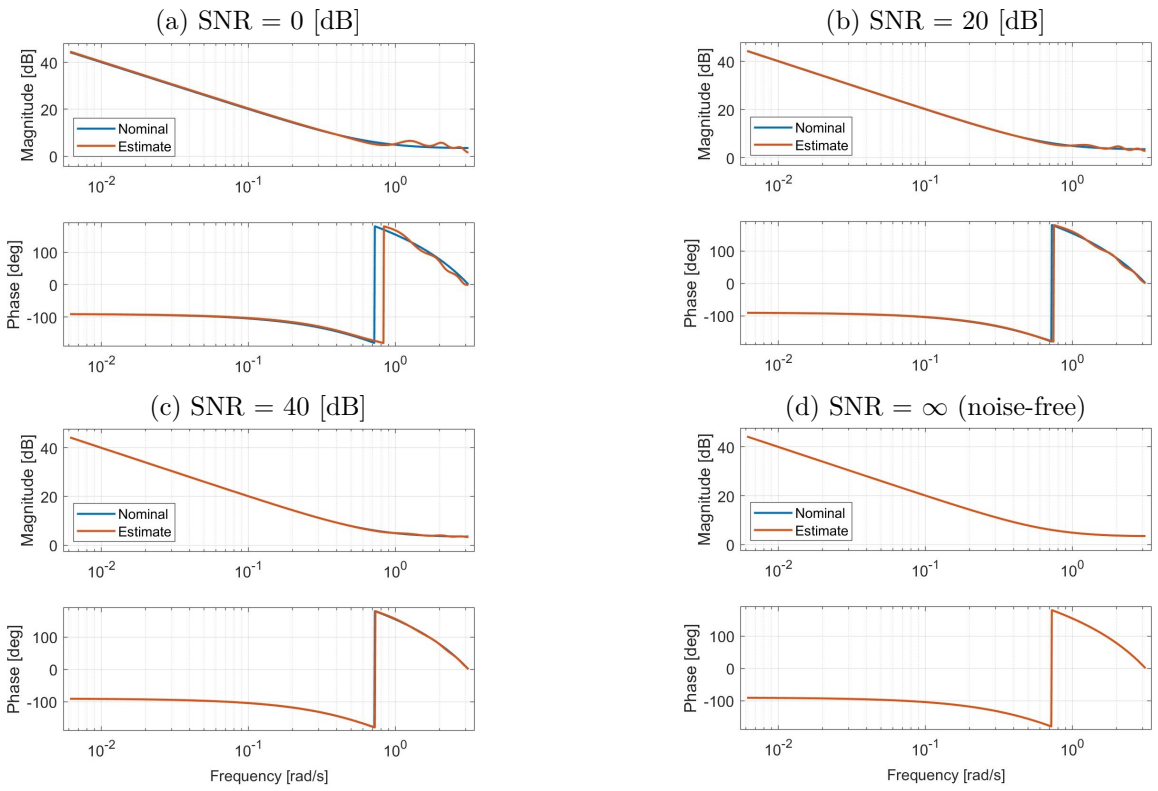

Figure 5.6: Bode diagram $\hat{\mathbf{G}}_{11}$ under different values of SNR and identical $N = 1023$.

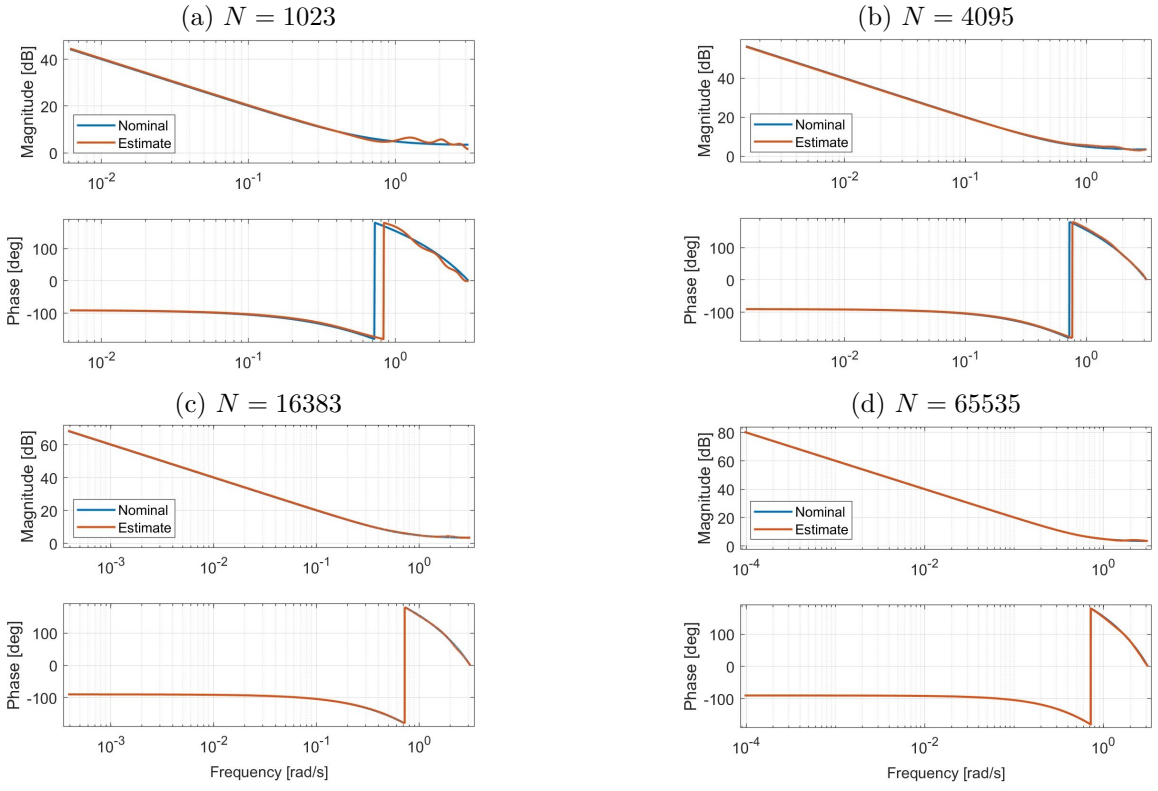

Figure 5.7: Bode diagram of $\hat{\mathbf{G}}_{11}$ under different values of N and identical SNR = 0 [dB].

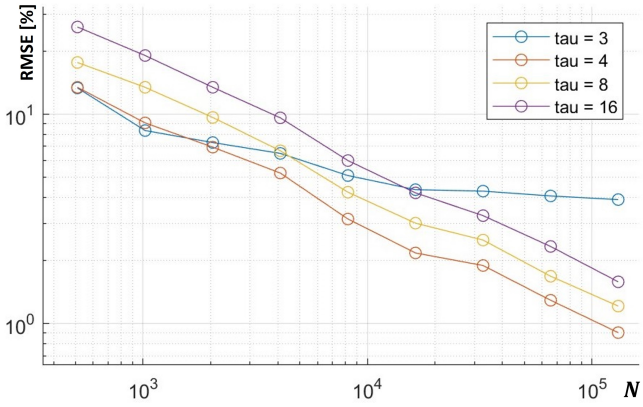

Figure 5.8: RMSE [%] vs. N and τ.

$N \setminus \tau$	3	4	8	16
511	13.3	13.4	17.6	26
1023	8.33	9.06	13.4	19
2047	7.3	6.94	9.62	13.4
4095	6.48	5.22	6.67	9.58
8191	5.08	3.15	4.23	5.99
16383	4.35	2.17	3.01	4.2
32767	4.28	1.89	2.5	3.27
65535	4.06	1.29	1.68	2.33
131071	3.9	0.904	1.21	1.58

Table 5.2: RMSE [%] vs. N and τ.

Clearly, $\tau = 4$ serves as a threshold for achieving an adequate order, ensuring the true model remains within the candidate set. The graphical representation illustrates that the estimate demonstrates consistency for $\tau = 4$, as the RMSE continuously decreases with increasing N. However, at $\tau = 3$, the RMSE converges to approximately 4% without further reduction. This observation indicates that $\tau = 3$ is insufficient to describe the model, thus leading to extra bias adequately. It is important to note that the model order τ is established for the Youla parameter $\mathbf{Q}$, which involves the closed-loop dynamics, thus generally possessing an order larger than that of $\mathbf{G}$. Furthermore, as the value of τ is raised, the RMSE curve shifts upward, even though it retains its asymptotic convergence concerning N. This phenomenon is likely attributed to an excessive model order resulting in overfitting the noise, subsequently increasing the estimate's variance. Notably, if we double the value of τ, the RMSE rises by approximately a factor of $\sqrt{2}$, which again coincides with Eq.5.20.

5.2.3 Estimates without Sparsity Constraints

As indicated by Eq.3.39, the variance associated with the constrained least-squares estimate is assuredly lower compared to the unconstrained estimate, provided the validity of the sparsity conditions. This variance reduction is regarded as an elevation in estimation efficiency, as the constrained estimate attains diminished variance or errors while requiring a smaller dataset. To visually illustrate this effect, we depict the Bode diagram of the estimated plant via unconstrained least-squares in Fig.5.9. Clearly, in the absence of sparsity constraints, the algorithm estimates the plant as one with a dense structure and allocates values to all channels, even those supposed to be zero. These arrangements result in an unnecessary estimate of the sparse channels, consequently worsening the non-sparse channels.

On the other hand, Fig.5.10 illustrates the variation in RMSE for the estimate without sparsity constraints, compared to that of the estimate with sparsity constraints. While the unconstrained RMSE showcases a consistent decrease with increasing data length, it always remains higher than the constrained counterpart under an identical experiment setup. Consequently, the constrained estimate outperforms the unconstrained one, thus worth consideration during optimization.
Therefore, through simulations, we have empirically verified that our proposed method is capable of achieving a decent estimate, by selecting an appropriate model order that is suitably larger than necessary rather than being excessively small. More importantly, applying the correct knowledge of sparsity conditions can help improve the sample efficiency as it significantly decreases the variance of the estimate. Still, it is possible to offer suggestions for improving the proposed method as part of future developments or reinforcing its theoretical underpinnings. These recommendations will be detailed in the conclusion chapter.

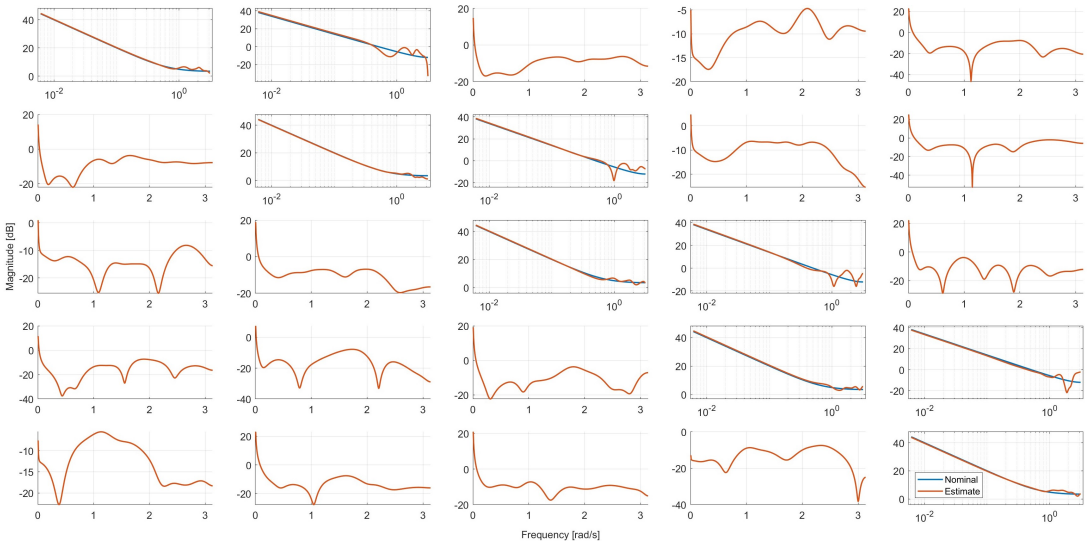

Figure 5.9: Magnitude response of the estimate without sparsity constraints, Given $N = 1023$, SNR $= 0$ [dB] and $\tau = 8$.

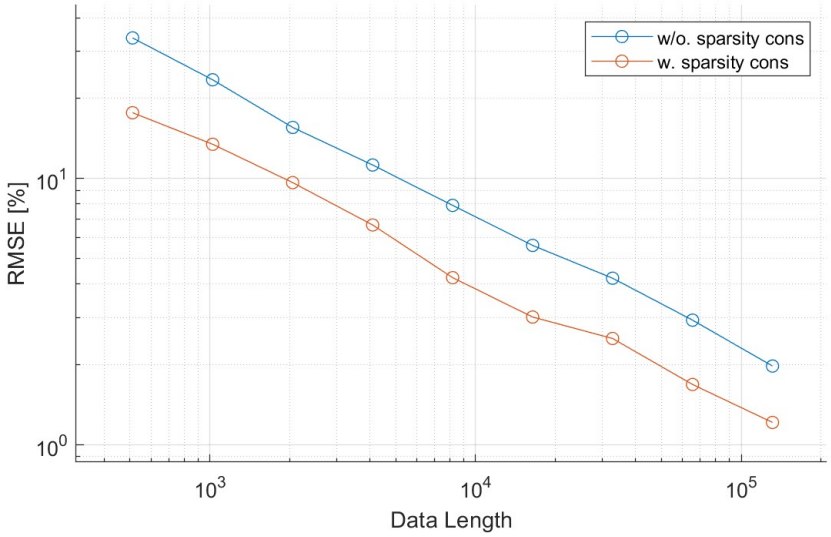

Figure 5.10: RMSE comparison between estimates with or without sparsity constraints.

Chapter 6

Conclusion and Future Works

We thereby summarize the report before providing several recommendations for future works. This project is motivated by increasingly extensive applications of modern cyber-physical systems (CPS), which may exhibit large-scale sparse architectures, unstable open-loop dynamics, and difficulty in building a representative model for controller synthesis. However, conventional closed-loop identification methods do not extensively deal with systems with sparsity structures, meaning the estimate can be relatively inefficient with slowly decreasing variance, or require a large number of redundant variables and data to develop a useful estimate. It thus becomes imperative to develop new techniques tailored for closed-loop identification of the CPS that effectively use sparsity knowledge and efficiently solve the large-scale identification problem.

With such purposes, we propose a novel idea that implements the Sparsity Invariance Theorem into system identification problems to make full use of the knowledge about the system's sparsity architecture to improve the estimate, compared with the original methods that do not utilize such a sparsity knowledge. We start with reviewing the Sparsity Invariance Theorem, which converts the inherently non-convex constraint on the sparsity structure of a factorizable transfer matrix into a pair of convex and sufficient conditions on its two factors. These conditions are named the Sparsity Constraints. Subsequently, we provide the derivation of the Stability Invertibility Theorem, according to which we can use a couple of linear constraints to ensure a transfer matrix has a stable and causal inverse without introducing extra unstable poles after inversion. However, these constraints can be further modified into a properly chosen regularizer, simplifying the problem while equivalently guaranteeing stable invertibility. These theorems lay the groundwork for understanding the convexification of several tricky constraints and ensuring the involved optimization problems are efficiently solvable.

Moving to the methodologies, we extend the theory of two typical closed-loop identification methods, namely the dual-Youla parameterization and the two-stage identification, from identifying linear time-invariant (LTI) single-input single-output (SISO) systems to multi-input multi-output (MIMO) systems, by adapting the sparsity constraints to utilize the information about the sparsity structure in the system. Both extended methods eventually result in a quadratic program that consists of a quadratic cost function that minimizes the model fitting error, and a group of linear equality constraints that ensure the estimated system has the desired sparsity structure. Such a program can be solved via either least-squares or instrumental variables and admit closed-form solutions. Considering the least-squares solution is much more efficient but biased, while the instrumental variables provide an unbiased and consistent estimate with increased computational complexity, it becomes a trade-off, and the selection between them should depend on the objective of the estimation.

Subsequently, we present an illustrative example of applying the identification framework to a real-world problem. An unstable and sparse irrigation network from the literature is chosen, which can be modeled as a large-scale LTI feedback control system, and stimulated by a sequence of pre-defined excitation reference signals, named training references. By collecting the resulting noisy data, from closed-loop operation, we subsequently employ these data to identify the underlying plant considering the sparsity architecture via the least squares estimate. Verification of the estimation is performed by exciting both the nominal and estimated systems with a sequence of validation references, which is statistically independent of the training references, collecting the validation outputs from the nominal system and predicted outputs from the estimated system, before computing the relative root mean squared error (RMSE) between these outputs. To further examine the properties of the identification framework, we run the algorithm in different scenarios, by varying the signal-to-noise ratio (SNR), the input data length, or the model order. Results indicated that RMSE gradually decreases to a relatively small level as we keep increasing the data length within a specific range. Raising the SNR also helps reduce the RMSE, with the reduction rate coinciding with the theories from the literature. In addition, the Bode diagrams visually show that the deviation between the estimated and nominal plants becomes nearly negligible as data length grows over 10^6 given an SNR of 0 decibels, resulting in an RMSE of merely about 1%. Despite the biases due to the least-squares method, we still achieve consistent output predictions and a commendable model approximation. Consequently, an appropriately chosen model order affects the estimate as well. We empirically show that an aggressively small model order can lead to obvious biases as the actual model is probably excluded from the candidate set. In contrast, an unnecessarily large model order will raise the estimate variance, hence increasing the prediction error. Conversely, if the model order is selected correctly, we are confident in concluding that the proposed method is verified and enabled to provide both satisfactory and efficient estimates.

Considering these facts, we would propose the following suggestions. As highlighted earlier in Section 3.3.4, the LS estimate is subject to bias and inconsistency when applied to estimating an ARMAX model as if it possesses an equation error structure. Despite these limitations, we continue to employ the LS estimate owing to its simple implementation and our initial objective of obtaining a representative approximation of the plant dynamics, rather than striving for consistent estimates of parameters. However, a desire exists to quantitatively determine the bias associated with the LS estimate, and explore potential strategies to mitigate this bias mathematically. Such quantification and mitigation are possible, as already addressed in [26], and this pursuit aims to enhance the accuracy of the estimation process. On the other hand, the ARMAX model can be consistently estimated by applying instrumental variables. Although a theoretical derivation has been provided in Section 3.3.4, we have not yet incorporated the IV estimate into our proposed method. Therefore, it is advisable to consider integrating the IV estimate in future work, enabling a comparison with the LS estimate in terms of consistency.

Beyond the choice of the estimator, the improvement of identification performance can also be pursued by strategically refining the experimental setup, as using PRBS signals is common but not necessarily optimal. PRBS signals possess uniform power spectral density across all frequencies, yet the irrigation system under consideration exhibits relatively slow dynamics, making high-frequency responses less valuable. In such cases, employing excitation signals specifically tailored for low frequencies could yield higher efficiency. Fortunately, alternatives have been proposed in [27] for identifying networked systems using prediction error methods; tailoring the excitation signals to the characteristics of the system dynamics makes achieving more efficient identification outcomes possible.

Last but not least, the approach taken in parameterizing the system can also be considered for improved estimation. The integration of the Sparsity Invariance Theorem can be extended to other parameterization methods that can make use of fractional representations. For instance, the system-level synthesis (SLS) technique[28] has proven to be a potent tool in controller design as it provides a reasonable parameterization of all stabilizing controllers and manages to convexify sparsity and communication constraints on the controller. Absolutely, the concept of SLS can be extended to closed-loop identification, which is denoted as the dual System-Level Parameterization as introduced in [29]. The author suggests that applying the dual-SLS framework to large-scale networks could be a promising direction for future research. Given this, incorporating the Sparsity Invariance Theorem into the dual-SLS parameterization for the identification of large-scale sparse networked systems appears to be worth investigating.

Meanwhile, another viable alternative is the Input-Output Parameterization (IOP) [30]. The IOP directly parametrizes the closed-loop transfer functions from external signals to control inputs and measured outputs, exploiting their affine relationship. This transformation enables the conversion of constraints on the closed-loop transfer functions into a convex formulation. Although, to our knowledge, the IOP concept has not been applied to system identification, the equivalence established among the Youla parameterization, system-level synthesis, and input-output parameterization[31] reveals the possibility that a similar framework can be developed for large-scale system identification using IOP.

In summary, these suggestions for future development together contribute to the improvement of the proposed method. By quantifying bias, exploring alternative estimation approaches, optimizing experimental setups, and refining parameterization techniques. Theoretically and practically, these recommendations can collectively improve the proposed technique, and the potential of achieving a more efficient and enhanced identification of large-scale sparse systems can be anticipated.

Bibliography

[1] L. Ljung. *System Identification: Theory for the User*. Prentice Hall information and system sciences series. Prentice Hall PTR, 1999.

[2] Paul Van den Hof. "Closed-loop issues in system identification". In: *Annual Reviews in Control* 22 (1998), pp. 173–186.

[3] Michel Gevers and Lennart Ljung. "Optimal experiment designs with respect to the intended model application". In: *Automatica* 22.5 (1986), pp. 543–554.

[4] Zhuquan Zang, Robert R Bitmead, and Michel Gevers. "Iterative weighted least-squares identification and weighted LQG control design". In: *Automatica* 31.11 (1995), pp. 1577–1594.

[5] P.G. Voulgaris. "A convex characterization of classes of problems in control with specific interaction and communication structures". In: *Proceedings of the 2001 American Control Conference. (Cat. No.01CH37148)*. Vol. 4. 2001, 3128–3133 vol.4.

[6] Su Ki Ooi, MPM Krutzen, and Erik Weyer. "On physical and data driven modelling of irrigation channels". In: *Control Engineering Practice* 13.4 (2005), pp. 461–471.

[7] Patricia Derler, Edward A. Lee, and Alberto Sangiovanni Vincentelli. "Modeling Cyber-Physical Systems". In: *Proceedings of the IEEE* 100.1 (2012), pp. 13–28.

[8] Florian Doerfler et al. "Sparsity-Promoting Optimal Wide-Area Control of Power Networks". In: *IEEE Transactions on Power Systems* 29.5 (2014), pp. 2281–2291.

[9] Fred Hansen, Gene Franklin, and Robert Kosut. "Closed-Loop Identification via the Fractional Representation: Experiment Design". In: *1989 American Control Conference*. 1989, pp. 1422–1427.

[10] P.M.J. Van den Hof, R.J.P. Schrama, and O.H. Bosgra. "An indirect method for transfer function estimation from closed loop data". In: (1992), 1702–1706 vol.2.

[11] Luca Furieri et al. "Sparsity invariance for convex design of distributed controllers". In: *IEEE Transactions on Control of Network Systems* 7.4 (2020), pp. 1836–1847.

[12] J. Adebayo et al. "Dynamical structure function identifiability conditions enabling signal structure reconstruction". In: *2012 IEEE 51st IEEE Conference on Decision and Control (CDC)*. 2012, pp. 4635–4641.

[13] Semyon Aranovich Gershgorin. "On the delimitation of the eigenvalues of a matrix". In: (1931).

[14] Mathukumalli Vidyasagar. *Control Systems Synthesis: A Factorization Approach*. MIT Press, 1988.

[15] Urban Forssell and Lennart Ljung. "Closed-loop identification revisited". In: *Automatica* 35.7 (1999), pp. 1215–1241.

[16] Thomas Kailath. *Linear Systems*. Prentice-Hall, Inc., Englewood Cliffs, N.J., 1980.

[17] EV Haynsworth. “On the Schur complement: Basel Mathematical Notes”. In: *University of Basel, BMN* 20 (1968).

[18] Trevor Hastie, Robert Tibshirani, and Martin Wainwright. *Statistical learning with sparsity: the lasso and generalizations*. CRC press, 2015.

[19] S.D. Fassois. “MIMO LMS-ARMAX Identification of Vibrating Structures - Part I: The Method”. In: *Mechanical Systems and Signal Processing* 15.4 (2001), pp. 723–735.

[20] T. Soderstrom and P. Stoica. “Comparison of some instrumental variable methods - Consistency and accuracy aspects”. In: *Automatica* 17.1 (1981), pp. 101–115.

[21] Andrzej Janczak. “Instrumental variables approach to identification of a class of MIMO Wiener systems”. In: *Nonlinear Dynamics* 48 (Jan. 2007), pp. 275–284.

[22] Xiaodong Cheng and JMA Scherpen. “Model reduction methods for complex network systems”. In: *Annual Review of Control, Robotics, and Autonomous Systems* 4 (2021), pp. 425–453.

[23] Sigurd Skogestad and Ian Postlethwaite. *Multivariable feedback control: analysis and design*. john Wiley & sons, 2005.

[24] Michael Cantoni et al. “Control of Large-Scale Irrigation Networks”. In: *Proceedings of the IEEE* 95.1 (2007), pp. 75–91.

[25] LászlóJ Naszódi. “On digital filtration in correlation time-of-flight spectrometry”. In: *Nuclear Instruments and Methods* 161.1 (1979), pp. 137–140.

[26] Wei Xing Zheng. “On Least-Squares Identification of ARMAX Models”. In: *IFAC Proceedings Volumes* 35.1 (2002). 15th IFAC World Congress, pp. 391–396.

[27] Arne Dankers et al. “Identification of Dynamic Models in Complex Networks With Prediction Error Methods: Predictor Input Selection”. In: *IEEE Transactions on Automatic Control* 61.4 (2016), pp. 937–952.

[28] James Anderson et al. “System level synthesis”. In: *Annual Reviews in Control* 47 (2019), pp. 364–393.

[29] Amber Srivastava et al. *A Dual System-Level Parameterization for Identification from Closed-Loop Data*. 2023.

[30] Luca Furieri et al. “An Input–Output Parametrization of Stabilizing Controllers: Amidst Youla and System Level Synthesis”. In: *IEEE Control Systems Letters* 3.4 (2019), pp. 1014–1019.

[31] Yang Zheng et al. “On the Equivalence of Youla, System-Level, and Input-Output Parameterizations”. In: *IEEE Transactions on Automatic Control* 66.1 (2021), pp. 413–420.

Eidgenössische Technische Hochschule Zürich
Swiss Federal Institute of Technology Zurich

Declaration of originality

The signed declaration of originality is a component of every semester paper, Bachelor's thesis, Master's thesis and any other degree paper undertaken during the course of studies, including the respective electronic versions.

Lecturers may also require a declaration of originality for other written papers compiled for their courses.

I hereby confirm that I am the sole author of the written work here enclosed and that I have compiled it in my own words. Parts excepted are corrections of form and content by the supervisor.

Title of work (in block letters):

Authored by (in block letters):
For papers written by groups the names of all authors are required.

Name(s):	**First name(s):**

With my signature I confirm that

- I have committed none of the forms of plagiarism described in the 'Citation etiquette' information sheet.
- I have documented all methods, data and processes truthfully.
- I have not manipulated any data.
- I have mentioned all persons who were significant facilitators of the work.

I am aware that the work may be screened electronically for plagiarism.

Place, date	**Signature(s)**

For papers written by groups the names of all authors are required. Their signatures collectively guarantee the entire content of the written paper.